frontiers in Marine Science

ORIGINAL RESEARCH
published: 22 October 2021
doi: 10.3389/fmars.2021.644094

Distribution and Abundances of Planktic Foraminifera and Shelled Pteropods During the Polar Night in the Sea-Ice Covered Northern Barents Sea

Katarzyna Zamelczyk[1,2], Agneta Fransson[1], Melissa Chierici[3], Elizabeth Jones[3], Julie Meilland[4], Griselda Anglada-Ortiz[5] and Helene Hodal Lødemel[3]*

[1] Norwegian Polar Institute, Fram Centre, Tromsø, Norway, [2] Department of Geosciences, UiT – The Arctic University of Norway, Tromsø, Norway, [3] Institute of Marine Research, Fram Centre, Tromsø, Norway, [4] MARUM – Center for Marine Environmental Sciences, University of Bremen, Bremen, Germany, [5] CAGE - Centre for Arctic Gas Hydrate, Environment and Climate, Department of Geosciences, UiT - The Arctic University of Norway, Tromsø, Norway

OPEN ACCESS

Edited by:
Stelios Katsanevakis, University of the Aegean, Greece

Reviewed by:
Katsunori Kimoto, Japan Agency for Marine-Earth Science and Technology (JAMSTEC), Japan
Brett Metcalfe, Wageningen University and Research, Netherlands

***Correspondence:**
Katarzyna Zamelczyk
Katarzyna.zamelczyk@uit.no

Specialty section:
This article was submitted to Marine Ecosystem Ecology, a section of the journal Frontiers in Marine Science

Received: *19 December 2020*
Accepted: *24 September 2021*
Published: *22 October 2021*

Citation:
Zamelczyk K, Fransson A, Chierici M, Jones E, Meilland J, Anglada-Ortiz G and Lødemel HH (2021) Distribution and Abundances of Planktic Foraminifera and Shelled Pteropods During the Polar Night in the Sea-Ice Covered Northern Barents Sea. Front. Mar. Sci. 8:644094. doi: 10.3389/fmars.2021.644094

Planktic foraminfera and shelled pteropods are important calcifying groups of zooplankton in all oceans. Their calcium carbonate shells are sensitive to changes in ocean carbonate chemistry predisposing them as an important indicator of ocean acidification. Moreover, planktic foraminfera and shelled pteropods contribute significantly to food webs and vertical flux of calcium carbonate in polar pelagic ecosystems. Here we provide, for the first time, information on the under-ice planktic foraminifera and shelled pteropod abundance, species composition and vertical distribution along a transect (82°–76°N) covering the Nansen Basin and the northern Barents Sea during the polar night in December 2019. The two groups of calcifiers were examined in different environments in the context of water masses, sea ice cover, and ocean chemistry (nutrients and carbonate system). The average abundance of planktic foraminifera under the sea-ice was low with the highest average abundance (2 ind. m^{-3}) close to the sea-ice margin. The maximum abundances of planktic foraminifera were concentrated at 20–50 m depth (4 and 7 ind. m^{-3}) in the Nansen Basin and at 80–100 m depth (13 ind. m^{-3}) close to the sea-ice margin. The highest average abundance (13 ind. m^{-3}) and the maximum abundance of pteropods (40 ind. m^{-3}) were found in the surface Polar Water at 0–20 m depth with very low temperatures (–1.9 to –1°C), low salinity (<34.4) and relatively low aragonite saturation of 1.43–1.68. The lowest aragonite saturation (<1.3) was observed in the bottom water in the northern Barents Sea. The species distribution of these calcifiers reflected the water mass distribution with subpolar species at locations and depths influenced by warm and saline Atlantic Water, and polar species in very cold and less saline Polar Water. The population of planktic foraminifera was represented by adults and juveniles of the polar species *Neogloboquadrina pachyderma* and the subpolar species *Turborotalita*

quinqueloba. The dominating polar pteropod species *Limacina helicina* was represented by the juvenile and veliger stages. This winter study offers a unique contribution to our understanding of the inter-seasonal variability of planktic foraminifera and shelled pteropods abundance, distribution and population size structure in the Arctic Ocean.

Keywords: planktic calcifiers, the Arctic ocean, winter aragonite and calcite saturation state, pH, nutrients

INTRODUCTION

Planktic foraminifera and shelled pteropods are groups of calcifying organisms that are ubiquitous in pelagic marine ecosystems (e.g., Beaugrand et al., 2009; Schiebel and Hemleben, 2017). These organisms are major pelagic producers of calcite and aragonite (most common forms of marine $CaCO_3$), respectively, and alongside coccolithophores play an important role in the ocean biogeochemical cycles and the organic and inorganic carbonate flux to the ocean floor (Milliman, 1993; Buitenhuis et al., 1996, 2019; Schiebel, 2002; Berelson et al., 2007). Planktic foraminifera provide 32–80% of the total calcite flux to the global deep ocean (Schiebel, 2002), whereas pteropods being more regionally and temporally variable, provide aragonite that may constitute up to ∼12% of the total carbonate flux globally (Berner and Honjo, 1981). In the polar areas, pteropods can provide > 50% of the carbonate flux to the interior of the ocean through the production of fecal pellets, mucous flocs and rapid post mortem settling of aragonite shells (Howard et al., 2011).

At polar latitudes the planktic foraminifera *Neogloboquadrina pachyderma* (Ehrenberg, 1861), *Turborotalita quinqueloba* (Natland, 1938) and pteropods *Limacina helicina* (Phipps, 1774), *Limacina retroversa* (Fleming, 1823) dominate their respective communities. *Neogloboquadrina pachyderma* and *L. helicina* are polar species recorded mainly in Polar waters, whereas *L. retroversa* and *T. quinqueloba* are considered to be subpolar species (Bathmann et al., 1991; Volkmann, 2000). The vertical and temporal distributions of planktic foraminifera and pteropods in spring and summer are suggested to be mainly determined by sea surface temperature and/or primary production in the surface waters (Bednaršek et al., 2012a; Schiebel and Hemleben, 2017). Regionally, these organisms constitute a significant part of total zooplankton biomass representing important grazers of primary producers and important prey for zooplanktivores (Lalli and Gilmer, 1989).

In recent years, planktic foraminifera and shelled pteropods have received widespread attention due to sensitivity to their $CaCO_3$ shells to ocean acidification (OA) (e.g., Comeau et al., 2009; Moy et al., 2009; Lischka et al., 2011; Lischka and Riebesell, 2012; Manno et al., 2012a,b, 2017; Bednaršek et al., 2014b, 2017, 2019; Bednaršek and Ohman, 2015). Responses of shelled pteropods (aragonite shell) to OA are documented as a declined growth rate and calcification of shell (Comeau et al., 2009, 2010; Lischka et al., 2011; Lischka and Riebesell, 2012; Bednaršek et al., 2014b) and the responses of planktic foraminifera (calcitic shell) to OA are still inconclusive (Kroeker et al., 2010; Manno et al., 2012a).

Despite their importance in the carbonate cycle, the impact of the carbonate chemistry variability on planktic foraminifera and shelled pteropod abundance and distribution is limited. It has been suggested that the mortality of pteropods increase as the seawater partial pressure of carbon dioxide (CO_2) increases, hence increasing the dissolution potential of $CaCO_3$, but the results of the few available experimental studies are uncertain and contradictory (Lischka et al., 2011; Comeau et al., 2012; Lischka and Riebesell, 2012). Until now, there is no clear evidence of a relationship between the carbonate chemistry variables and the abundance and distribution of these planktic calcifiers in the natural environment.

During the Arctic winter, the ocean's carbonate chemistry shifts toward the highest pCO_2, lowest pH and saturation states for $CaCO_3$ (Ω) due to increased CO_2 solubility during cooling, increased CO_2 from respiration of organic matter, and intensification of wind-induced vertical mixing of high-CO_2 subsurface water (e.g., Fransson et al., 2017). All these processes cause decreases in the calcite (Ω_{Ca}) and aragonite saturation (Ω_{Ar}) states (e.g., Chierici et al., 2011; Shadwick et al., 2011; Fransson et al., 2017). Moreover, the progressing oceanic uptake of atmospheric CO_2 will reduce the carbonate ion concentration thereby shifting the marine CO_2 system toward increased concentrations of bicarbonate ions. This reduces both the ocean's buffering capacity for further CO_2 uptake and the degree of $CaCO_3$ saturation, simultaneously increasing the solubility of $CaCO_3$ minerals (Zeebe and Wolf-Gladrow, 2001 and references therein).

It is still under debate if Arctic pteropods, such as *Limacina helicina*, slow down their metabolism and growth during wintertime or continue the metabolic activity (Lischka and Riebesell, 2012; Berge et al., 2020; Thibodeau et al., 2020). Furthermore, a recent study from the west Antarctic Peninsula has shown evidence that *Limacina helicina antarctica* shells actively grow during the ice-covered winter season with continued growth into the summer (Thibodeau et al., 2020). The overwintering strategy is suggested to exert a domineering impact on the ability of pteropods to counteract changes in their environment. Polar and subpolar pteropods and planktic foraminifera species are mainly feeding on available particulate matter, with a diet of phytoplankton in spring and summer and degraded organic material in late autumn and winter (Gannefors et al., 2005; Schiebel and Hemleben, 2017). The ability to feed on dead organic matter probably allows them to increase their survival potential in winter.

Knowledge regarding planktic foraminifera during the polar night is poor, apart from a few studies in the Southern Ocean documenting the ability of *N. pachyderma* to overwinter in brine channels in pack and fast ice (Dieckmann et al., 1991; Spindler, 1996). In the Barents Sea, studies of planktic foraminifera and pteropods including abundances, vertical and temporal

distribution and the overall importance of these species in the marine ecosystems are scarce and restricted to a few studies from the southern and central parts (Kacprzak et al., 2017; Pasternak et al., 2017; Meilland et al., 2020; Ofstad et al., 2020). Moreover, all the studies focus on data obtained from spring to autumn. Until now, no winter data on the abundance and depth distribution of planktic foraminifera and shelled pteropods in the seasonally sea-ice covered northern Barents Sea exist.

The aim of this study is to provide new information linking under-ice planktic foraminifera and pteropods abundances, their species and size distributions to water depth and contrasting water masses during the Arctic winter. We examine the range of environmental variables and explore possible environmental preferences of these small calcifying zooplankton species along a north-south transect in the northern Barents Sea and the Nansen Basin. The results are discussed in the context of sea-ice cover, water masses, food limitation, nutrients, pH, Ω_{Ca} and Ω_{Ar}. Additionally, we discuss the potential contribution of these calcifiers to the organic and inorganic carbon flux during the polar night.

Study Area

The general oceanic circulation pattern in the Barents Sea is shown in **Figure 1A**. The relatively warm and saline Atlantic Water (AW) enters the Barents Sea mainly from the southwest at the Barents Sea Opening, where the West Spitsbergen Current (WSC) bifurcates into two main branches (Loeng, 1991). As the WSC flows northward through the eastern Fram Strait entering the Arctic Ocean, a fraction of the AW follows the Eurasian continental margin into the central Arctic Ocean, where the AW enters the Barents Sea from northwest as a subsurface inflow (e.g., Mosby, 1938; Lind and Ingvaldsen, 2012; **Figures 1A,B**). The warm and saline AW and the cold Polar Water (PW) are separated by the Polar Front characterized by strong temperature and salinity gradients and differences in seasonal sea-ice cover.

In the northern Barents Sea, the PW isolates the sea-ice cover from the subsurface AW. Along the way, the AW is gradually mixed with PW creating a modified AW (mAW) (Pfirman et al., 1994). The PW consist of the remnants of the mixed water formed by cooling and brine rejection in winter (Rudels et al., 1996). The main supply of freshwater for the winter mixed water in the northern Barents Sea is sea-ice import from the Nansen Basin and adjacent Kara Sea in addition to precipitation (Rudels et al., 2004). The Barents Sea Deep Water (BSDW) is formed locally through ice freezing and thermohaline convective processes as well as the modification of AW through atmospheric cooling (e.g., Lien and Trofimov, 2013).

The seasonal variability of the marine CO_2 system and nutrients in the Barents Sea follows the physical and biological processes (Reigstad et al., 2002). The nutrient uptake is initiated by the spring bloom, which continues to late summer, leading to nitrate depletion and low CO_2 levels (high Ω and pH) in the surface waters due to photosynthetic activity by phytoplankton. By fall, the nutrient and CO_2 values increases due to the mixing of nutrient and CO_2 rich sub-surface waters to the surface water. Biological processes (photosynthesis and respiration) are postulated to explain much of the observed seasonal changes of the carbonate/CO_2 system in the Arctic Ocean as well as on the air-sea CO_2 exchange (Chierici et al., 2011; Tynan et al., 2016; Fransson et al., 2017).

The sea-ice conditions in the Barents Sea show a high seasonal and inter-annual variability (e.g., Deser et al., 2000; Vinje, 2001; Shapiro et al., 2003; Divine and Dick, 2006). Generally, the ice conditions are influenced by Atlantic and Polar Water masses, the import of sea-ice from the north and by atmospheric conditions. Usually, sea-ice coverage is at a minimum in September, whereas maximum sea-ice cover typically occurs in April (Norwegian Meteorological Institute, 2020). During our winter sampling, the sea-ice concentration decreased from north (∼110 cm) to south (∼20 cm) and only the southernmost station was ice-free (**Figure 1C**).

MATERIALS AND METHODS

The research was conducted in the northern Barents Sea between 82°3′50′ N, 28°30′6′ E and 76°0′ N, 31°13′8′ E in December 2019 aboard the Norwegian icebreaking R/V *Kronprins Haakon* within the Nansen Legacy project (**Figure 1**).

Water column temperature and salinity profiles (**Figure 2**) were obtained with a conductivity-temperature-depth (CTD) sensor system Sea-Bird SBE 911 + mounted on a General Oceanic rosette sampler equipped with 24 Niskin bottles used for seawater sampling of chemical variables in the water column.

Seawater samples for the macronutrients nitrate [NO_3^-], phosphate [PO_4^{3-}], and silicic acid [$Si(OH)_4$] were drawn from the Niskin bottles into 20 mL vials, preserved with chloroform and stored at 4°C. Analysis were carried out using a Flow Solution IV analyzer from O.I. Analytical, United States, following Grasshof et al. (2009) at the Institute of Marine Research, Bergen, Norway. The analyzer was calibrated using reference seawater from Ocean Scientific International Ltd., United Kingdom. The detection limits were 0.04 mmol m^{-3} for [NO_3^-] and 0.06 mmol m^{-3} for [PO_4^{3-}].

Seawater samples for total dissolved inorganic carbon (DIC) and pH were collected following standard procedures outlined in Dickson et al. (2007) and subsequently analyzed within approximately 24-hrs at a temperature around 25°C. pH was measured on the total hydrogen scale (pHT) using spectrophotometric determination according to Clayton and Byrne (1993) and the indicator dye, meta-cresol purple. The perturbation of the sample pH due to the dye addition was corrected according to Chierici et al. (1999). The precision was generally better than 0.001 units as determined from the average standard deviation for triplicate measurements. DIC was determined using a coulometric titration with a Versatile Instrument for the Determination of Titration Alkalinity (VINDTA 3D, Marianda, Germany). The procedure is described in Dickson et al. (2007). Routine analyses of Certified Reference Materials (CRM, provided by A. G. Dickson, Scripps Institution of Oceanography, United States) ensured the accuracy and precision of the DIC measurements. The average standard deviation from triplicate CRM analyses was within ± 2 μmol kg^{-1}.

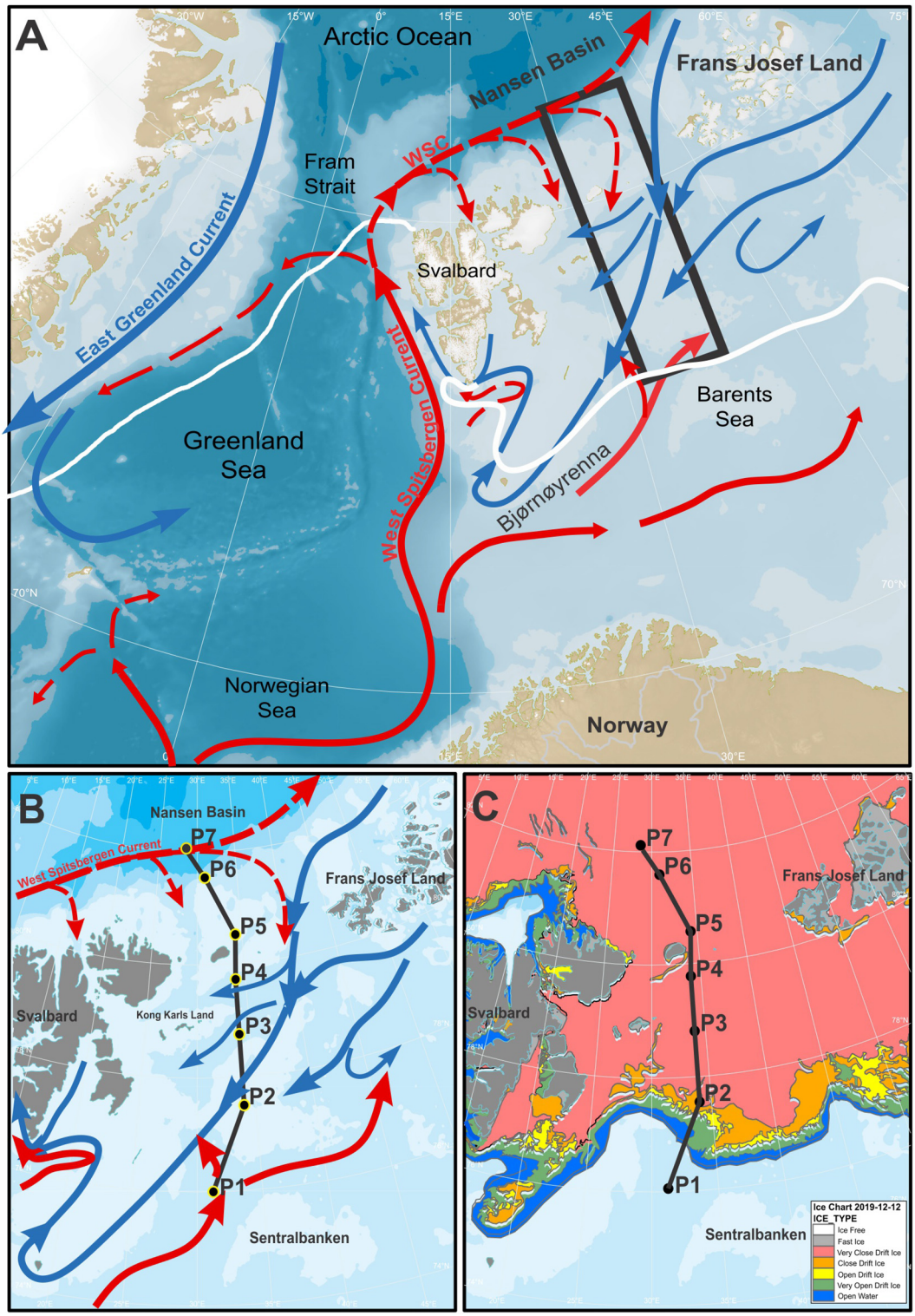

FIGURE 1 | (A) Schematic map of the main current systems in the Nordic Seas and the Barents Sea. The study area is indicated by a black rectangle. The Polar Front is indicated by a white line. Solid and dashed red/blue lines show surface and subsurface ocean currents, respectively. **(B)** Oceanic currents in the study area and **(C)** sea-ice extension, sea-ice type of the last day of sampling (12th December 2019). The transect of sampled stations is shown as black line. The sea ice map was generated using GSHHG (Global Self-consistent, Hierarchical, High-resolution Geography Database) data from the Norwegian Meteorological Institute and ice data were provided by the Norwegian Ice Service (MET Norway).

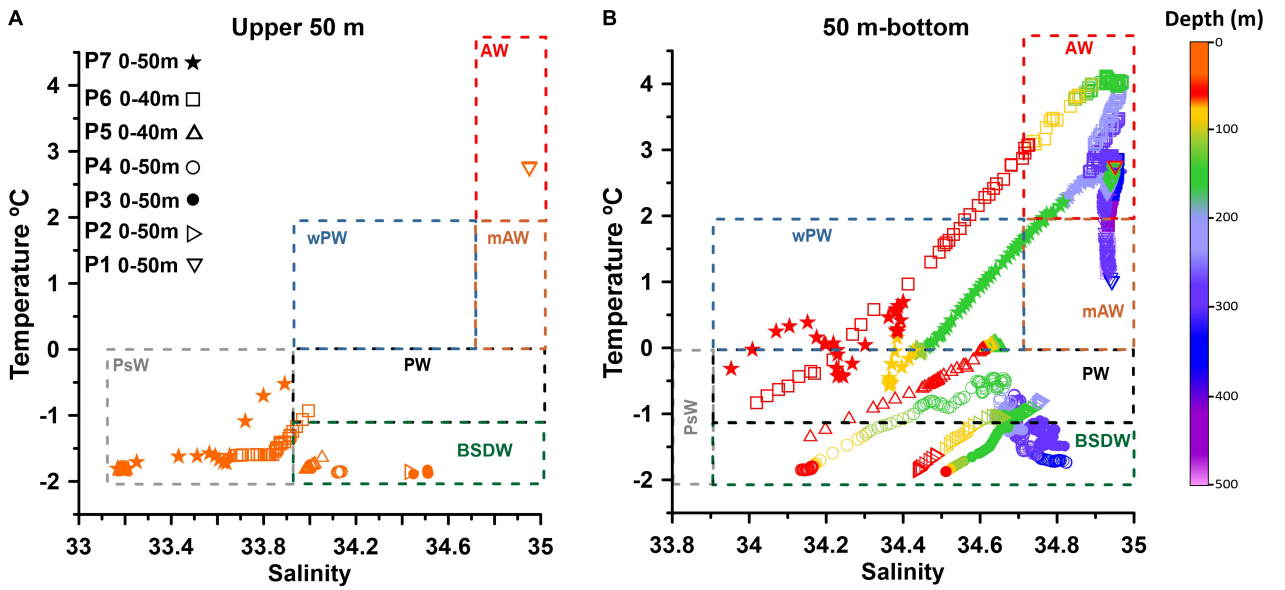

FIGURE 2 | The temperature-salinity characteristics of water masses based on the CTD profiles at **(A)** 0–50 m water depth and **(B)** from 50 m water depth to near-bottom in December 2019 at each station (symbol-coded). PsW- Polar surface Water, PW- Polar Water; wPW- warm Polar Water, AW- Atlantic Water, mAW- modified AW, BSDW- Barents Sea Deep Water (Sundfjord et al., 2020 with a slight modification). The data for deeper stations P7 and P6 (**Table 1**) are shown only for the upper 300 m of the water column.

The *in situ* pH and $CaCO_3$ saturation states of aragonite (Ω_{Ar}) and calcite (Ω_{Ca}) were calculated from pairs of DIC and measured pH, together with the temperature, salinity, pressure, $Si(OH)_4$] and [PO_4^{3-}] using the chemical speciation model CO2SYS (Pierrot et al., 2006). The carbonic acid dissociation constants of Mehrbach et al. (1973) as refitted by Dickson and Millero (1987) were used in combination with the bisulfate dissociation constant from Dickson (1990), and the total boron concentration of Lee et al. (2010). The aragonite and calcite stoichiometric solubility constants of Mucci (1983) were used with the pressure corrections of Millero (1979) and the calcium concentration and salinity ratio of Riley and Tongudai (1967).

Planktic foraminifera and shelled pteropods were collected at seven stations (P7 to P1) along a north-south transect (**Figures 1B,C** and **Table 1**) using a stratified plankton tow (MultiNet Hydro-Bios type Midi, opening of 0.25 m^2) equipped with five net bags with 63 μm mesh gauze. Sampling was performed at each station immediately after or before the CTD cast. One vertical haul sampled five depth intervals (**Table 1**) from the back of the ship except for station P7 and P1, where the sampling was performed *via* the moonpool inside the research vessel. Depth intervals 0–20, 20–50 m were sampled at each station. Deeper depth intervals were determined by the bathymetry at each station, with last depth interval close to the sea floor except for station P7 (3,517 m water depth), where only the upper 300 m were sampled (**Table 1**). Samples at station P6, P4 and P2 were analyzed immediately after recovery on board and samples at station P7, P5, P3 and P1 were frozen at −80°C until processing on land, at the NPI/IMR Fram Center laboratory, Tromsø, Norway. The content of each cod-end was concentrated on a cascade of 500, 250, 100 and 63 μm meshed sieves and segregated with stream of sea water into size ranges: > 500, 500–250, 250–100, 100–63 μm. All planktic foraminifera and pteropods were counted for each size range separately, and, if applicable, identified to species level under a microscope [Leica M60 (on board); Leica M80 (on land)] equipped with transmitted light bases (**Supplementary Table 1**). In addition, the diameter of pteropods > 500 μm was measured (**Supplementary Table 2** and **Supplementary Figure 1**). The majority of taxa was identified to species level morphologically. However, individuals in the smallest size ranges could not be assigned to species as they lacked the morphological features characteristic for specific species. This ambiguity occurred mainly for planktic foraminifera in size range 100–63 μm and for pteropods in size range 250–63 μm that subsequently were termed as planktic foraminifera juveniles and small-sized *Limacina* (ssL), respectively. Planktic foraminifera species in range size 250–100 μm are considered as adults (Brummer et al., 1986; Caromel et al., 2016). Pteropods in size ranges > 500, 500–250, 250–100 μm were classified according to Lalli and Gilmer (1989) with slight modifications. Life stages in our study are defined as follows: adults (>4,000 μm for *L. helicina* and > 1,000 μm for *L. retroversa*), juveniles (for *L. helicina* 4,000–500 μm and for *L. retroversa* 1,000–500 μm), early juveniles-late veligers (500–250 μm), veligers (250–100 μm) and early veligers (100–63 μm). Following the size metric of pteropods generally used in the literature the size of *L. helicina*, *L. retroversa* and ssL will be reported in millimeters (mm) hereafter.

Living (cytoplasm bearing) and dead (empty shells) pteropods and foraminifera were distinguished *via* the presence or absence of cytoplasm/soft body visible through the shell, respectively. Shells with degraded remnants of soft tissues were considered as

TABLE 1 | Sampling locations, temperature and salinity ranges and tow information at each (P) station. Asterisk (*) indicates ice-free station.

St.	Long. N	Lati. E	Sampling date	Water depth (m)	Temp. (°C) min max	Salinity min max	Depth sampled (m)	Filtered water volume (m^3)
P7	82° 3′ 50″	28° 30′ 6″	2019-12-2	3,517	−1.81 2.70	33.19 34.96	0–20	8
							20–50	11
							50–100	18
							100–200	34
							200–300	34
P6	81° 32′ 32″	30° 56′ 46″	2019-12-5	844	−1.60 4.12	33.68 34.97	0–20	8
							20–50	11
							50–200	51
							200–600	100
							600–750	84
P5	80° 31′ 2″	34° 16′ 25″	2019-12-6	143	−1.82 0.09	33.98 34.65	0–20	8
							20–50	11
							50–80	11
							80–100	8
							100–125	10
P4	79° 43′ 30″	33° 59′ 28″	2019-12-8	344	−1.86 −0.46	34.12 34.77	0–20	8
							20–50	11
							50–100	18
							100–200	34
							200–300	34
P3	78° 45′ 0″	33° 59′ 35″	2019-12-9	305	−1.89 −1.10	34.45 34.79	0–20	8
							20–50	11
							50–100	18
							100–200	34
							200–280	28
P2	77° 30′ 0″	34° 0′ 7″	2019-12-10	190	−1.86 −0.80	34.37 34.76	0–20	8
							20–50	11
							50–80	11
							80–100	8
							100–170	24
P1*	76° 0′ 0″	31° 13′ 8″	2019-12-12	326	2.74 0.97	34.92 34.95	0–20	8
							20–50	11
							50–100	18
							100–200	34
							200–300	34

dead and only shells with a clearly visible soft body were counted as living. As the net was trawled vertically, samples volumes (m^3) were calculated from the net mouth area and deployed depth range (m). Results are given in absolute abundances in number of individuals per cubic meter of filtered water (ind. m^{-3}).

RESULTS

Physical and Chemical Characteristics of the Water Masses

Water mass identifications are based on the temperature-salinity characteristics measured in December 2019 (**Figures 2A,B**). The water mass definitions follow Sundfjord et al. (2020) with a slight modification. At each station covered by sea-ice (P7–P2, **Figure 1C**) a cold (near or at freezing temperatures), relatively fresh and homogenous under-ice Polar surface Water (PsW) layer was observed (**Figures 2A**, **3B**, **4B**). The depth of the PsW layer varied between 10 and 60 m. Warm and saline AW was found below the PsW at station P7, P6 and at the station P1. Below the AW layer, a mAW and warm Polar Water (wPW) was identified (**Figures 2**, **3B**, **4B**). The core of Atlantic water (identified by the subsurface temperature maximum) was observed at P7 at ∼210 m and at P6 at ∼138 m water depths. At station P5, below the surface layer, colder and less saline PW was found (**Figures 2**, **3B**, **4B**). At stations P4, P3 and P2, below the very cold (<−0.4°C) and relatively low salinity PsW (34.12–34.76), cold and more saline PW was recorded. At greater depths, vertical temperature (T < −1.1°C) and salinity (> 34.5) gradients indicate

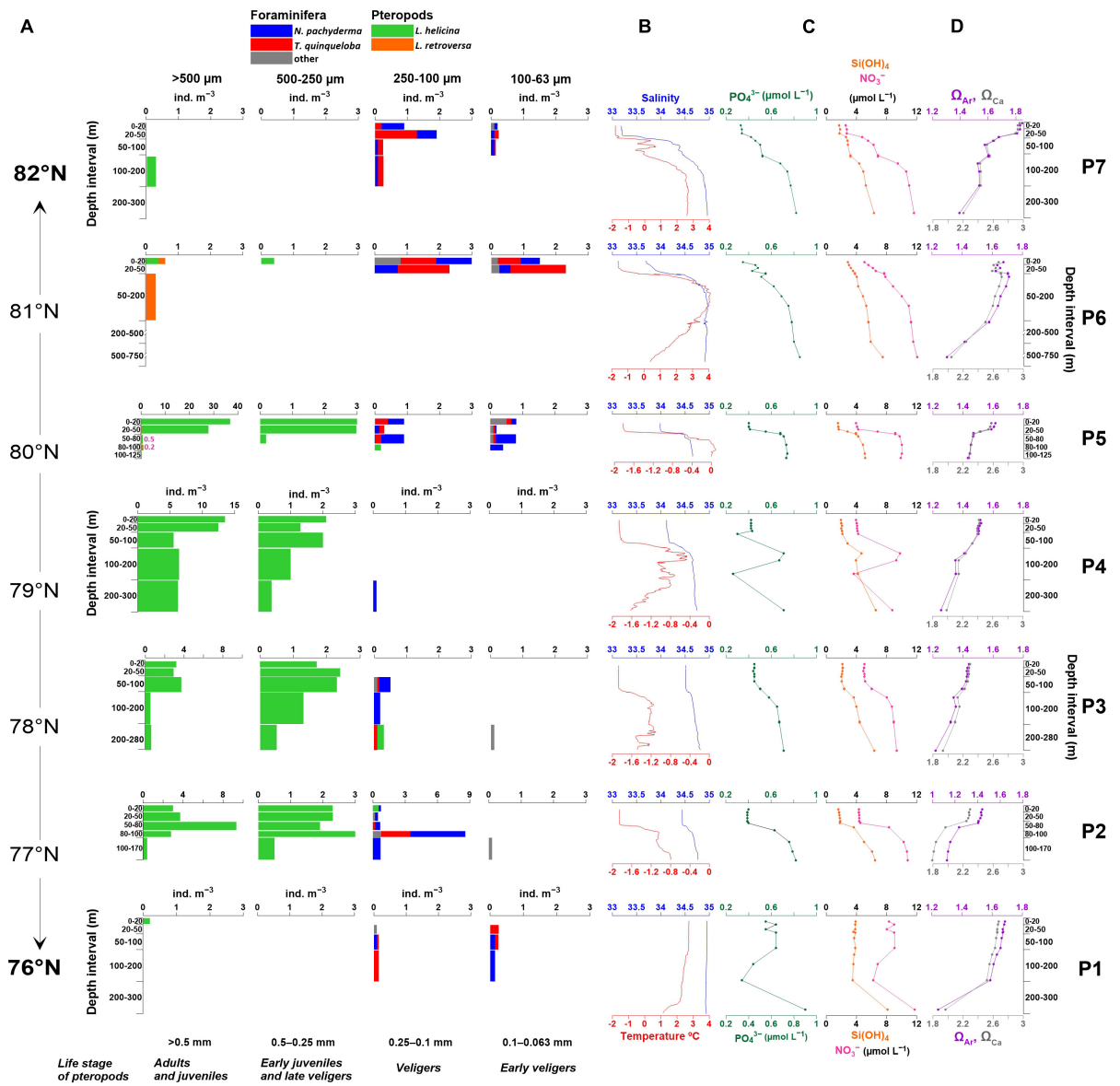

FIGURE 3 | (A) Absolute abundances (ind. m^{-3}) and size distribution of living planktic foraminifera and pteropods species plotted against sampled depth intervals. Numbers in pink at station P5 indicate abundances of *Clione limacine*. **(B)** temperature and salinity (from 10 m water depth), **(C)** inorganic nutrients concentrations (PO_4^{3-}, $Si(OH)_4$, NO_3^-), **(D)** aragonite (Ω_{Ar}) and calcite (Ω_{Ca}) saturation state at each station. Note different x-axis for the abundance in size range 250–100 µm at station P2 and for size range > 500 µm at stations P2-P5. Temperature, salinity, nutrients, Ω_{Ar} and Ω_{Ca} at station P7 are shown for the upper 300 m of the water column.

the occurrence of BSDW at these stations (**Figures 2**, **3B**, **4B**). The surface water (upper ∼100 m) of the sea-ice free station P1 was occupied by warm (2.71–3.63°C) and saline (34.95–34.79) AW. Below 100 m depth, cooler and less saline mAW with temperature < 2°C and average salinity of 34.94 were found (**Figures 2**, **3B**, **4B**).

The distribution of carbonate chemistry variables varies both between the stations along the transect and within the vertical gradient of the water columns (**Table 2** and **Figures 3D**, **4C**). The Ω values decreased from the surface to the bottom waters. Both Ω_{Ar} and Ω_{Ca} were oversaturated ($\Omega > 1$) throughout the entire water column at all stations (**Figures 3D**, **4C**). The maximum values (Ω_{Ar} = 1.85 and Ω_{Ca} = 2.95) were recorded in the surface water at the northernmost station P7 and the minimum values (Ω_{Ar} = 1.13 and Ω_{Ca} = 1.79) at station P2 close to the sea floor at ∼180 m water depth (**Table 2** and **Figures 3D**, **4C**). The maximum pH of 8.25 was recorded at the surface at station P7 and the minimum pH of 7.99 at the bottom at station P2 (**Table 2**).

The highest concentrations of all nutrients were recorded below 100 m at stations P6 and P2 (**Table 2** and **Figure 3C**). Maximum concentrations of the different nutrients were

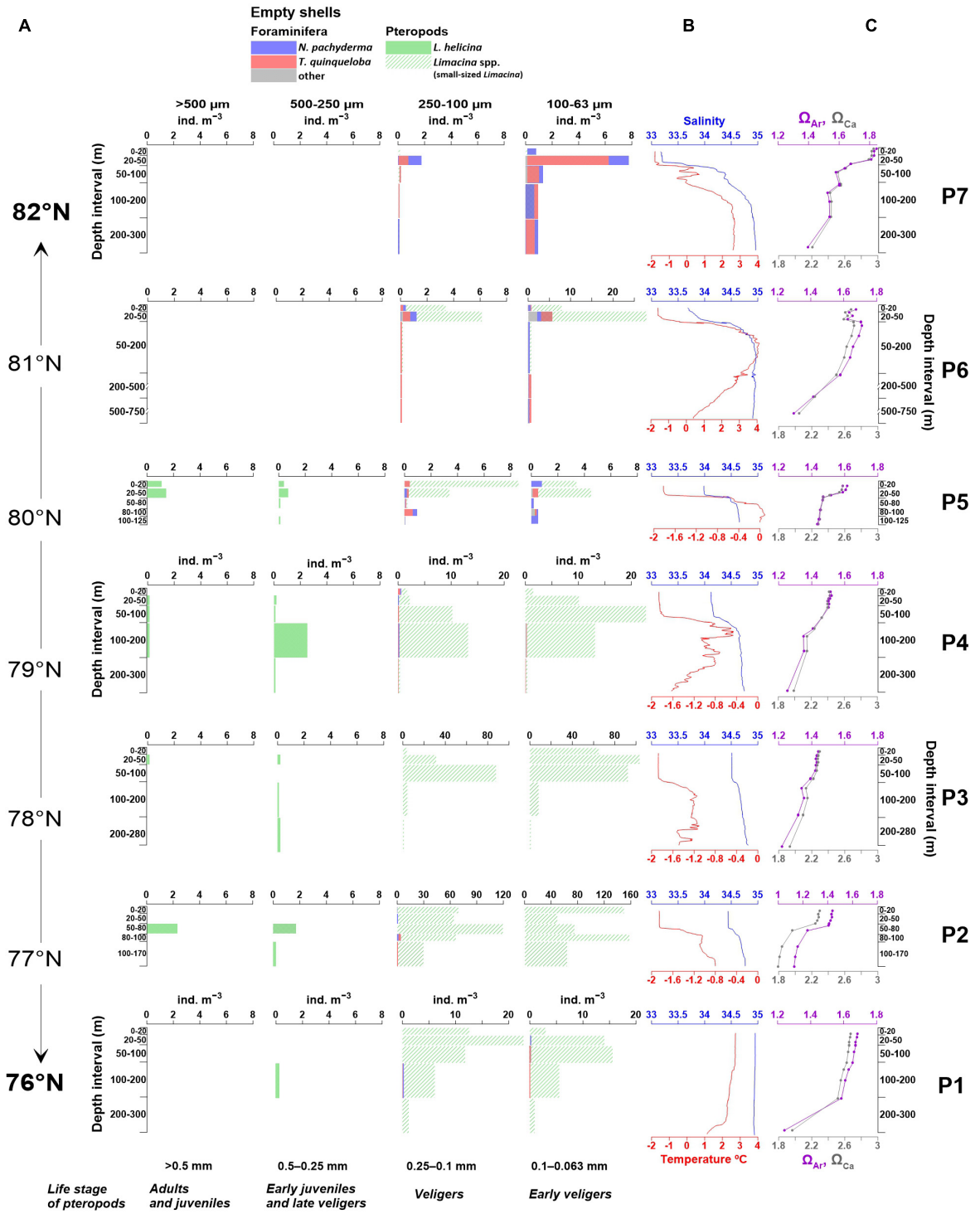

FIGURE 4 | (A) Absolute abundances (ind. m^{-3}) and size distribution of dead planktic foraminifera and pteropods species **(B)** temperature and salinity (from 10 m water depth) and **(C)** aragonite (Ω_{Ar}) and calcite (Ω_{Ca}) saturation state at each station plotted against sampled depth intervals. Note different x-axis for the abundance in size ranges 250–100 µm and 100–63 µm. Temperature, salinity, Ω_{Ar} and Ω_{Ca} at station P7 are shown for the upper 300 m of the water column.

~11 µmol L^{-1} for [NO_3^-], 6.5 µmol L^{-1} for [$Si(OH)_4$] and ~0.8 µmol L^{-1} for [PO_4^{3-}]. The lowest concentrations were observed in the surface water at station P7 with 2.6 µmol L^{-1} of [NO_3^-], 1.7 µmol L^{-1} of [$Si(OH)_4$] and 0.3 µmol L^{-1} of [PO_4^{3-}] (**Table 2** and **Figure 3C**). The low concentrations of nutrients and Ω ware mainly found in the PW (stations P4, P3,

TABLE 2 | Carbonate chemistry, degree of $CaCO_3$ saturation (Ω_{Ar}, Ω_{Ca}) and pH, inorganic nutrient concentrations (µmol L^{-1}) in the water column.

Para-meter	P7*		P6		P5		P4		P3		P2		P1	
	Range	Mean ± SD	Range	Mean ± SD	Range	Mean ± SD	Range	Mean ± SD	Range	Mean ± SD	Range	Mean ± SD	Range	Mean ± SD
Ω_{Ar}	1.40–1.85	1.65 ± 0.15	1.26–1.71	1.58 ± 0.15	1.43–1.61	1.51 ± 0.07	1.25–1.52	1.44 ± 0.09	1.22–1.44	1.38 ± 0.07	1.13–1.44	1.32 ± 0.14	1.24–1.68	1.61 ± 0.13
Ω_{Ca}	2.21–2.95	2.62 ± 0.25	1.98–2.71	2.50 ± 0.25	2.28–2.57	2.40 ± 0.12	1.99–2.43	2.29 ± 0.14	1.93–2.30	2.19 ± 0.11	1.79–2.29	2.10 ± 0.22	1.96–2.67	2.56 ± 0.20
pH	8.05–8.25	8.15 ± 0.08	8.04–8.19	8.09 ± 0.05	8.07–8.17	8.11 ± 0.04	8.05–8.14	8.10 ± 0.03	8.03–8.10	8.07 ± 0.02	7.97–8.10	8.05 ± 0.06	7.99–8.08	8.07 ± 0.03
NO_3^-	2.6–13.8	9.31 ± 4.3	5.1–12.7	8.94 ± 2.6	4.0–10.0	7.54 ± 2.8	3.9–9.8	5.59 ± 2.6	4.9–9.3	6.47 ± 1.9	4.3–10.8	6.63 ± 3.0	6.2–11.7	8.51 ± 1.7
$Si(OH)_4$	1.7–12.4	6.3 ± 4.0	2.9–8.9	4.82 ± 1.79	1.5–5.1	3.42 ± 1.54	1.9–6.5	3.12 ± 1.52	2.0–6.4	3.02 ± 1.42	1.6–6.5	3.16 ± 1.97	3.5–8.1	4.13 ± 1.32
PO_4^{3-}	0.33–0.97	0.70 ± 0.25	0.35–0.9	0.62 ± 0.18	0.4–0.74	0.59 ± 0.15	0.3–0.71	0.48 ± 0.16	0.45–0.71	0.53 ± 0.10	0.39–0.82	0.54 ± 0.19	0.34–0.9	0.58 ± 0.16

Ranges of each variable, average values and standard deviation recorded from the whole water column at each station are given.
(*) indicates values and averages for upper 300 m water depth.

P2) and the relatively high nutrients and Ω concentrations are observed in the AW mass and its admixture.

Abundance and Species Distribution of Living Planktic Foraminifera and Pteropods

Living planktic foraminifera integrated for the upper 200 m of the water column was generally very low with highest abundance of 2.3 ind. m^{-3} recorded at station P2 where water depth was 170 m (**Figure 5**). At the northernmost stations, planktic foraminifera were found in the upper 50 m of the water column with abundances reaching up to 2.6 ind. m^{-3} at station P7 and 6.8 ind. m^{-3} at station P6. At P5, the distribution was rather uniform within the upper 100 m of the water column. At station P2, the highest abundance of planktic foraminifera of 2.3 ind. m^{-3} occurred in the deeper between 50 and 170 m water depth (**Figure 3A**). The polar species *N. pachyderma* dominated at all stations except for station P6 and P1 where the subpolar species *T. quinqueloba* dominated (**Figure 5**).

Highest average abundance of pteropods was observed at station P5 (12.5 ind. m^{-3}) where the abundance was estimated for the upper 125 m water depth and P4 (8.5 ind. m^{-3}) where the abundance was estimated for the 0–200 m interval of the water column (**Figure 5**). Pteropods were absent or close to absent at AW influenced stations such as stations P7 and P1 (**Supplementary Table 1**). The polar species *L. helicina* dominated at all stations (100%) except for station P6 and P5 where the subpolar species *L. retroversa* was still low (0.3 ind. m^{-3} and 0.2 ind. m^{-3}) but constituted 80 and 1.2% of the total pteropod relative abundance, respectively (**Figure 5**). At station P5, the majority of *L. helicina* were distributed in the upper 50 m of the water column and at stations P4 and P3 the depth distribution of this species was rather uniform, coinciding with the distribution of the PW (**Figures 3A,B**). At station P2, most of this species occurred below 50 m water depth (**Figure 3A**). While living ssL (0.25–0.063 mm) were scarce, early juveniles-late veligers of *L. helicina* (0.5–0.25 mm) accounted for > 35% of the total abundance at all stations of occurrence (**Figure 3A**). Vertical distribution of juveniles of *L. retroversa* (>0.5 mm) at station P6 and P5 was also limited to upper 50 m water depth. Adults of *L. retroversa* (> 1 mm) were found at stations P6 and P5 in the upper 20 m of the water column and at the 50–100 m water depth interval. *Clione limacina* that is known as the predator of *L. helicina* (Lalli, 1970; Conover and Lalli, 1974; Norekian and Satterlie, 1996; Böer et al., 2005) was recorded only at station P5 (0.13 ind. m^{-3}) at 20–50 and 80–100 m water depth with abundances of 0.5 ind. m^{-3} and 0.2 ind. m^{-3}, respectively (**Figure 3A**).

Abundance and Species Distribution of Dead Planktic Foraminifera and Pteropods

The concentration of dead planktic foraminifera (empty shells) in the upper 200 m water depth varied between

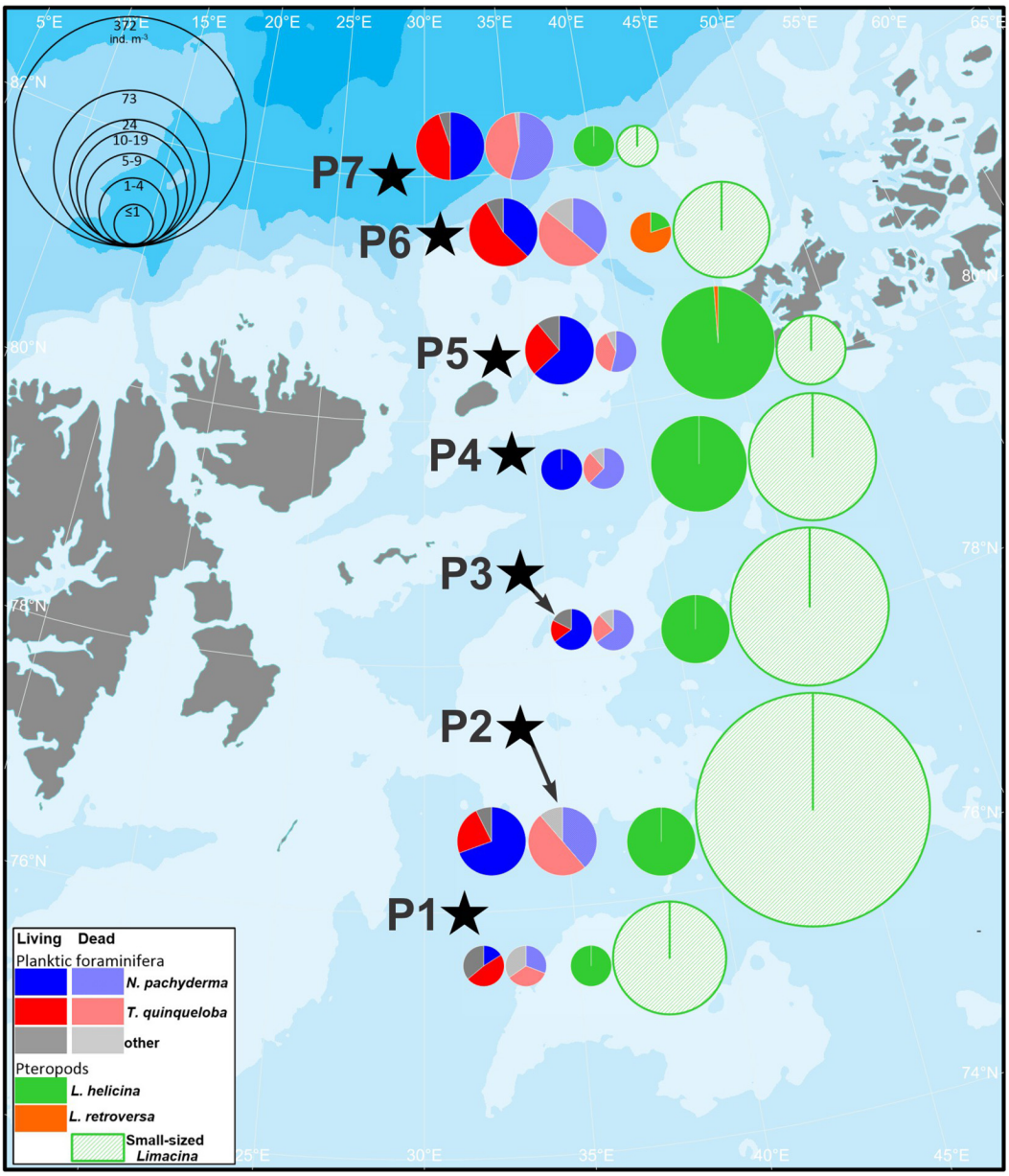

FIGURE 5 | Distribution of living and dead species of planktic foraminiferal and pteropods along the north-south transect in the northern Barents Sea. All data are presented for the upper 200 m water depth except for station P2 and P5 where the water depth is 170 m and 125 m, respectively. Species are color-coded and indicated in the legend. Total abundance (ind. m^{-3}) of living (real colors) and dead (dimmed colors) planktic foraminifera and pteropods are indicated by the size of the pie charts with a legend in the left corner. Sampling locations are indicated by black stars. Small-sized *Limacina* includes empty shells of *Limacina* spp. in size fraction 250–63 μm not identifiable to species level.

0.4 ind. m^{-3} (stations P1, P3) and 3.7 ind. m^{-3} (station P7) (**Figure 5**).

The concentration of dead pteropods varied between 0.1 ind. m^{-3} (within 0–200 m) at station P7 and 372 ind. m^{-3} at station P2 (within 0–170 m) (**Figure 5**). Between 95% and 98% of dead pteropods accounted for the ssL in size range 0.25–0.1 mm and 0.1–0.063 mm, respectively (**Figure 4A**). Dead specimens in size fraction > 0.25 mm were represented only by the *L. helicina* species (**Figure 5**).

DISCUSSION

Oceanic Factors Influencing Abundances of Living Planktic Foraminifera, Shelled Pteropods and Concentration of Their Empty Shells

Advection and mixing by ocean currents are the primary physical forcing experienced by marine organisms and therefore

of a great concern in plankton studies. The contribution of transported zooplankton to the Arctic Ocean has not yet been adequately quantified and is hence poorly defined (Wassmann et al., 2015). Although, shelled pteropods are active swimmers and planktic foraminifera are able to regulate their buoyancy *via* cellular components and thus inhabit certain depths (Marszalek, 1982; Schiebel and Hemleben, 2017), their abundances can be influenced by the direction and intensity of ocean currents. Lateral advection may transport shells of planktic foraminifera over distances of > 25 km for *N. pachyderma* and > 50 km for *T. quinqueloba* (Von Gyldenfeldt et al., 2000). Transport of shells can also be strengthened by water stratification that increases resident time at the shear boundary between water masses (Kuhnt et al., 2013). As the northern Barents Sea has a complex hydrography (**Figure 1**), the extension of lateral advection of planktic foraminifera and shelled pteropods is poorly constrained. However, considering potential lateral advection of planktic foraminiferal shells, Pados and Spielhagen (2014) observed, that in an equally dynamic area such as the deep Fram Strait, the distribution pattern discerned by plankton tows was clearly reflected on the sediment surface strongly suggesting that the effect of ocean currents on planktic foraminifera is negligible. As the veligers of shelled pteropods are only slightly smaller and comparable in size to planktic foraminifera, the assumption can be valid for the ssL too. In addition, the wind-driven ocean circulation, mixing and the resulting strengthening of surface currents, that could potentially facilitate the transport of small planktic foraminifera and pteropods shells, is significantly subdued due to the presence the sea-ice cover during our sampling time. Moreover, the velocities of ocean currents in the Barents Sea are very low, with bottom currents ranging between 2 and 3 cm s^{-1} (e.g., Kushnir et al., 2007) and surface currents oscillating around an average of 1.8 cm s^{-1} (Abrahamsen et al., 2006). Therefore, the lateral transport of planktic foraminifera and pteropods, although possible, can be considered as insignificant. This is evident in the species composition of pteropods along the transect, except for the northern station P5, where the mean currents velocities are reported to be higher up to 10 cm s^{-1} (Lind and Ingvaldsen, 2012). The presence of the few subpolar pteropod *L. retroversa* and the slightly higher temperature at station P5, compared to stations P4–P2 located within the PW regime, suggest that the lateral southward transport of this species by the admixture of AW masses from station P6, where the highest abundance of *L. retroversa* was recorded, is very likely (**Supplementary Table 1** and **Figures 3A,B**, **5**).

In case of dead shells, in addition to physical environmental factors that in the study area during our sampling time likely are inconsequential, the sinking speed of empty dead shells may be decisive for their residence time in the surface water. The sinking speeds of planktic foraminifera shells are governed by shell weight, volume and presence or absence of spines. The sinking speed of the spinose species, e.g., *T. quinqueloba* is approximately threefold slower than those of the non-spinose species (Caromel et al., 2014). Based on data from plankton tows most planktic foraminifera > 150 μm sink at speeds of 13.3–53 m h^{-1} (Takahashi and Bé, 1984). Similarly to planktic foraminifera, the sinking behavior of shelled pteropods is also strongly correlated to their shell morphology and size, with the tiny coiled shell pteropods sinking the slowest, the large globular shelled pteropods sinking the fastest, and the medium-sized elongated shell pteropods sinking at intermediate speeds (Walker et al., 2021). The sinking velocity of empty pteropod shells was approximated between 36 and 50 m h^{-1} (Lalli and Gilmer, 1989) and the sinking speed for *L. helicina* was estimated to 18–162 m h^{-1} (Chang and Yen, 2012). The rather fast sinking velocities of empty shells of planktic foraminifera and pteropods imply a short retention time in the surface waters and quick settlement upon death. Considering the distances between and water depths at our stations, the average sinking speed for *L. helicina* of 90 m h^{-1} (Chang and Yen, 2012) and the average current speed of 65 m h^{-1} (Abrahamsen et al., 2006), it is unlikely that the empty shells has been transported by currents at station P4–P1. Moreover, most of the dead shells found in our samples, still contained fragments of the soft tissue that was visible through the transparent shells. The presence of the incompletely degraded remnants of organic matter in the shells indicate that the organisms likely recently died and thus represent a population that lived and/or survived under-ice conditions until the sampling time in the area.

Living Planktic Foraminifera

Only one study on living planktic foraminifera from the central-northern Barents Sea area has been undertaken (Ofstad et al., 2020) and knowledge regarding the seasonal distribution of planktic foraminifera in the polar regions is still scarce. Until now, no data of under-ice planktic foraminifera fauna from the Arctic winter are available. In the northern Barents Sea, the average abundance of under-ice planktic foraminifera were low and occurred mainly in the upper 50 m of the water column (P7—P5, **Figure 3A**). In April (2016) in the year-round ice-free Bjørnøyrenna area, ∼235 km south of our southernmost station (P1), the average concentration of planktic foraminifera ranged from 0 to 6 ind. m^{-3} (Ofstad et al., 2020). Moreover, abundances of <10 ind. m^{-3} have been reported at Bjørnøyrenna Trough in summer (Meilland et al., 2020). The similarly low abundances recorded in winter (December), spring and summer suggest that sea-ice cover and low temperatures do not significantly influence the abundance of planktic foraminifera. This coincides with recent results from the south-west Barents Sea showing that in shallow waters the commonly attributed environmental parameters such as temperature and salinity have limited influence on the abundance of planktic foraminifera (Schiebel and Hemleben, 2017; Meilland et al., 2020). Shallow depths may impede the production of planktic foraminifera (Schmuker, 2000), which therefore likely and partially can explain the observed low abundance in the shallow Barents Sea.

The under-ice species composition recorded along the transect shows that *T. quinqueloba* constitutes from 18 to 67% of the total planktic foraminiferal fauna (**Figures 3A**, **5**). Given previous studies that consider *N. pachyderma* as the dominant species in polar regions, making up more than 90% of the total planktic foraminiferal assemblages (Kucera et al., 2005; Pados and Spielhagen, 2014), the relatively high proportion of *T. quinqueloba* in the high north is somewhat surprising.

In addition, *T. quinqueloba* is found alive in water masses with temperatures below 0°C suggesting a potential adaptation of this subpolar foraminifera to the conditions in the area (**Figures 3A**, **5**). However, for a true species shift to occur, the organism must be able to reproduce in the new environment. Despite the occurrence of juveniles (100–63 μm) in the area (**Figure 3A**), *in situ* reproduction cannot be proven with our data. Moreover, the relatively high numbers of dead juveniles (0.2–7.5 ind. m^{-3}, **Figure 4A**), compared to living juveniles (0.1–2.3 ind. m^{-3}, **Figure 3A**), suggest a noteworthy mortality at stations P7–P5. This implies that these organisms can survive rather than adapt to the under-ice conditions. The survival and future presence of subpolar planktic foraminifera in the under-ice waters in winter can be associated with the ability of these organisms to feed on a wide variety of food including dead organic matter (Schiebel and Hemleben, 2017) that may be stored in young sea-ice (Gradinger and Ikävalko, 1998; Krembs et al., 2002) and upon melting released to the under-ice water. In winter, sea-ice may serve as a storage of dead organic matter from the previous productive season.

Living Shelled Pteropods

The concentrations of under-ice abundance of living pteropods (0.1–12.5 ind. m^{-3}, **Figure 5**) in our study in the northern Barents Sea in winter are relatively comparable to under-ice concentrations of 0.4–179 ind. m^{-3} observed at 0 and 5 m water depth in late winter upon return of daylight (March) in Storfjorden (Werner, 2005). Surprisingly, they are also similar to concentrations recorded in spring (0–5 ind. m^{-3} in April) and in summer (0–47 ind. m^{-3} in June) reported for 0–300 m water depth in central Barents Sea (Bjørnøyrenna) (Ofstad et al., 2020). During the peak reproduction time in August-September the average abundance of pteropods in the upper ∼300 m varied between 3 and 851 ind. m^{-3} north of Svalbard (Daase and Eiane, 2007) and between 13 and 52 ind. m^{-3} at the average depth of 122 m in the central and southern parts of the western Barents Sea (Kacprzak et al., 2017). The abundances of pteropods over the Barents Sea-Svalbard area may also reflect the patchiness of their occurrence, as they locally are able to form dense aggregations in the water column (Percy and Fife, 1985).

In our study, the dominant polar species *L. helicina* was confined to the cold PW supporting previous results that indicate a connection between pteropod abundances and certain water mass properties in the western Barents Sea (Kacprzak et al., 2017). The highest abundance of 65.2 ind. m^{-3} was observed at 0–50 m water depth at station P5 in very cold water masses with temperatures of –1.8 to –1°C (**Figures 3A,B**). The high abundances of *L. helicina* followed the distribution of the very cold water at station P4 that extended to the sea bed from 50 m water depth (**Figures 3A,B**).

The relation of pteropods to certain water masses in winter is also observed, alike planktic foraminifera (see above), in the species composition of pteropods. The highest percentage of the subpolar pteropod *L. retroversa* (80%, 0.9 ind. m^{-3}) was found in AW masses with the warmest temperatures of 3.0–4.1°C and the highest recorded salinity of 34.9 at station P6 (**Figures 3A,B**, **5**). These warm temperatures agree with the optimal temperature tolerance of 2.0–16°C previously reported for *L. retroversa* (van Der Spoel, 1967, 1976). The water temperature in which *L. helicina* was found, ranges between –2°C and 0°C and it is lower than the previously assessed temperature tolerance of –0.4°C and +4.0°C (van Der Spoel, 1967, 1976). This may suggest that *L. helicina*, as the subpolar planktic foraminiferal species *T. quinqueloba*, adapted to and/or survived the very low temperatures *in situ* under the sea-ice cover in the northern Barents Sea. The life cycle of planktic foraminifera in high latitudes in winter is still unknown and the overwintering strategy of pteropods is still under debate (Lischka and Riebesell, 2012; Berge et al., 2020; Thibodeau et al., 2020). Independent from, whether pteropods live in a stage of reduced metabolism (Lischka and Riebesell, 2012) or the overwintering strategy is no change in metabolism with a continued active growth (Berge et al., 2020; Thibodeau et al., 2020), they are able to adapt to and survive harsh conditions of the under-ice waters.

Relationship of Living Pteropods With Environmental Parameters

The surface waters of the Arctic Ocean with low temperatures and naturally low Ω_{Ar} (Chierici and Fransson, 2009) are expected to become locally undersaturated with respect to aragonite within a decade (Steinacher et al., 2009). Yet, undersaturated waters have been found already in summer 2005 on freshwater influenced Arctic shelves (Chierici and Fransson, 2009). Although the Ω_{Ar}, Ω_{Ca} and pH were low in the water column along the transect in the northern Barents Sea, the Ω_{Ar} and Ω_{Ca} values did not attain undersaturation with values < 1 (**Table 2** and **Figure 3D**). However, Ω_{Ar} of 1.23–1.13 recorded at station P2 already between 90 and ∼180 m water depth and < 1.3 in the deepest water masses at stations P1, P3 and P4 are very low in comparison with other winter-spring data available in literature for the Barents Sea region (Chierici et al., 2019; Ofstad et al., 2020; **Table 2** and **Figure 3D**). Moreover, these Ω_{Ar} values (<1.4) are reported to be critical for *L. helicina* shell formation (Bednaršek and Ohman, 2015; Bednaršek et al., 2019). The Ω_{Ar} values recorded at station P2 fall < 1.2, which is a threshold under which shell calcification of this species can be greatly reduced (Bednaršek et al., 2017). Although it has been suggested that *L. helicina* can precipitate aragonite at $\Omega_{Ar} < 1$ (at temperature ∼4°C), the shell dissolution is reported to continue (Comeau et al., 2010). In a future climate change with more meltwater and continued anthropogenic CO_2 uptake resulting in decreased Ω_{Ar} values, it is likely that *L. helicina* in the northern Barents Sea will experience larger stress and will require more energy to avoid shell dissolution and continue shell growth. This could compromise the fitness (Fabry et al., 2008), threaten their survival (Comeau et al., 2011; Bednaršek et al., 2012a; Maas et al., 2012) and possibly influence the abundances and distribution of these planktic calcifiers. Moreover, environmental parameters in the northern Barents Sea, show strong covariance between the ocean carbonate chemistry, temperature, salinity and nutrients within each station (**Figures 3B–D**). Therefore, a single environmental parameter cannot be selected as main variable influencing abundances and distribution of these planktic calcifiers. In addition to food availability,

the ocean variables could independently or simultaneously intensify or counterbalance the environmental impact on the abundance and distribution of planktic foraminifera and shelled pteropods in our study.

Population Size Structure and Life Cycle

Because of the relatively small size of planktic foraminifera and the difficulties to maintain live specimens in laboratory cultures during complete a life cycle (Murray, 1991), estimates of foraminiferal longevity and life cycles are still debated (Nigam et al., 2003). The life span estimates are very variable ranging from a few days to almost 8 months (e.g., Caron and Swanberg, 1990; Spindler, 1996; Nigam et al., 2003). Primary production and food availability have been suggested to define the suitable conditions for growth and reproduction of planktic foraminifera (Kretschmer et al., 2016). When sufficient food is accessible, planktic foraminifera can attain maturity by quickly adding the last few chambers and undergo gametogenesis. The relatively high under-ice abundances of living juveniles (0.1–0.063 mm) observed in the northern Barents Sea during winter may represent a population of overwintering juveniles spawned just before the sea-ice thickened that survived under the sea-ice by feeding on marine snow (**Figure 3A**).

Pteropods were represented by *L. helicina* juveniles (>0.5 mm) and late veligers (0.5–0.25 mm) and by the male form of *L. retroversa* (> 1 mm, Lalli and Gilmer, 1989; **Supplementary Table 2**). The size structure alongside the abundance of pteropods is commonly used to estimate the rate of growth and determine their life cycle. There is an increasing number of studies discussing the life cycle of pteropods, among which the life cycle of *L. helicina* is of special interest (e.g., Gannefors et al., 2005; Hunt et al., 2010; Wang et al., 2017). Due to environmental conditions, especially primary productivity (Seibel and Dierssen, 2003) and seawater temperature (Seibel et al., 2007, 2012; Lischka et al., 2011), wide regional variations in the life cycle model for *L. helicina* have been presented.

In Kongsfjorden (Svalbard) (Gannefors et al., 2005) and in the north Pacific (Wang et al., 2017) spawning of *L. helicina* took place in spring and autumn. The longevity in these areas was proposed to be 1 year (Gannefors et al., 2005). In the high Arctic Ocean, Kobayashi (1974) observed a prolonged spawning period between later winter and late autumn and suggested a longevity of 1.5–2 years. In addition, two contrasting life cycles are presented for *L. helicina* in the Southern Ocean where both a 1-year (Hunt et al., 2008) and a 3-year longevity (Bednaršek et al., 2012a) has been proposed.

The abundance and size range of *L. helicina* found in December in the northern Barents Sea suggest that the juveniles (4.0–0.5 mm) of this species likely represent the population that was spawned in late autumn. This coincides with studies from the Arctic Ocean and Svalbard fjords that suggest a breeding period of *L. helicina* during autumn (Kobayashi, 1974; Gannefors et al., 2005). Recently, an active grow of *Limacina helicina antarctica* has been reported throughout the winter season in the Southern Ocean (Thibodeau et al., 2020). Therefore, it is possible that the occurrence of living juveniles in December may indicate that a growth of the overwintering *L. helicina* (veligers into juveniles) occurred despite of the lack of daylight (hence limited primary production), the increase and thickening of sea-ice cover and declining food quality during early winter months (October to December). The ongoing growth during winter months can probably be linked to the ability of veligers of *L. helicina* to feed on poor nutritional choices, which, during winter, can be limited to degraded organic material (Kobayashi, 1974; Gannefors et al., 2005), as is also suggested for planktic foraminifera (see above). In addition, juveniles of *L. helicina* can accumulate lipids and utilize them in winter (Gannefors et al., 2005; Boissonnot et al., 2019).

Furthermore, the absence of living young veligers in the size range 0.25–0.1 mm and 0.1–0.063 mm in December indicates either that no spawning occurred in early winter (October-December) or that the veligers of *L. helicina* did not survive the early stage of their development (**Figure 3A**).

The highest abundance of juvenile *L. helicina* was observed at 0–20 m (37 ind. m^{-3}) and at 20–50 m (28 ind. m^{-3}) water depth at station P5 (**Figures 3A,B**). The occurrence in surface waters is in agreement with studies from the central Arctic, Svalbard fjords and Barents Sea where migration of juveniles and veligers of *L. helicna* was observed in the top 75 m (Kobayashi, 1974; Gannefors et al., 2005; Falk-Petersen et al., 2008; Ofstad et al., 2020). We speculate that locally occurring enhanced food availability such as sea-ice-associated microalgae aggregates and/or release of degraded organic material originating from summer and autumn blooms, possibly caused the high concentration in the upper water column at this station.

Overall, the abundances of two groups of pelagic calcifiers, their population size structure and species distribution appear to be the result of a complex interplay of ecological factors and roles in the marine food web. For instance, *L. helicina*, like other pteropods (and unlike planktic foraminifera), has the ability to actively migrate in the water column and our data represent a snapshot-type observation that cannot provide a comprehensive picture of the dynamics of planktic foraminifera and pteropods nor the environmental factors controlling their populations. In addition, comparisons of pteropod abundances to other studies can bear discrepancies that often can be attributed to use of different plankton net mesh sizes (e.g., Kacprzak et al., 2017 - > 500 μm; Gannefors et al., 2005 - > 180 and > 1,000 μm; Daase and Eiane, 2007 - > 180 μm). Pteropod abundance reported with mesh size greater than those of our study, the study from central Barents Sea (> 0.63 μm) (Ofstad et al., 2020) and from Storfjorden (> 0.50 μm, Werner, 2005) is, therefore, incomplete or represent a different plankton community. Moreover, a repeated sampling strategy covering full annual cycles would be crucial for studying long-term trends in the occurrence, abundance and population structure of planktic foraminifera and shelled pteropods to improve our understanding and prediction of their sensitivities to ocean changes.

Biological Carbon Flux and Empty Shells

Planktic foraminifera and pteropods are involved in numerous pathways of carbon export from the surface (where they live) to the ocean floor (where they settle after death). They contribute

to carbon export primarily *via* their shells as an inorganic carbon flux (Heinze et al., 1991) and their soft-tissue/cytoplasm as an organic carbon flux (Volk and Hoffert, 1985). The two carbon exports mechanisms contribute to the biological carbon pump that draws down atmospheric CO_2 through production of organic matter and subsequently sequesters the particulate organic carbon exported to the deep ocean (Volk and Hoffert, 1985). Planktic foraminifera and shelled pteropods also contribute to the carbonate counter pump that counteracts the biological carbon pump by increasing surface ocean CO_2 through calcification and precipitation of calcite and aragonite shells and the resulting export of particulate inorganic carbon out of the surface layer. The balance between the biological carbon pump and the carbonate counter pump regulates the efficiency of deep ocean CO_2 sequestration and, as a consequence, affects the concentrations of CO_2 in the surface ocean and influences air-sea CO_2 exchange.

Contrary to pteropods, organic carbon flux of soft tissue (i.e., cytoplasm) of planktic foraminiferal has so far been assumed to be very low (e.g., Watanabe et al., 2014; Meilland et al., 2018), as sedimentation of planktic foraminifera occurs primarily as empty shells with little to no remaining cytoplasm. In the case of pteropods, the contribution to the carbon flux can additionally occur *via* production of fecal pellets or fast sinking colloids that are formed while feeding *via* mucous webs that trap fine particles and small fecal pellets (Howard et al., 2011).

The biogeochemical importance of calcite and aragonite production by planktic foraminifera and pteropods, respectively, and their importance for carbon flux has been discussed on global and regional scales in a great number of studies (e.g., Milliman, 1993; Schiebel, 2002; Tyrrell, 2008; Bednaršek et al., 2012a; Schiebel and Hemleben, 2017; Manno et al., 2018; Meilland et al., 2018; Buitenhuis et al., 2019). Most of these studies based the assessment of organic and inorganic carbon flux on the quantification of living assemblages, whereas the concentration and quantification of empty shells of planktic foraminifera and pteropods and thus the potential significance for especially the inorganic carbon flux record, have gone often unreported.

In the northern Barents Sea, the concentrations of empty shells exceeded the concentration of living individuals, or in case of planktic foraminifera, are close to equal at each station except for station P5 (**Figure 5**). Given the low absolute abundances of planktic foraminifera in our study (**Figure 5**), in this chapter we focus mainly on empty shells of pteropods. At the southernmost station (P1) no living pteropods were observed and the concentration of empty shells of 19 ind. m^{-3} was recorded. North of the Polar Front, at station P2 and P3 the concentration of empty shells was almost 93-fold and 19-fold higher, respectively, than the concentration of living pteropods showing a density of 372 ind. m^{-3} and 73 ind. m^{-3}, respectively (**Figure 5**). Although, the largest portion of the empty shells of pteropods were recorded in the smallest size range of 0.25–0.063 mm, the concentration is rather significant.

The causes of mortality of natural plankton populations are extremely difficult to determine, particularly, in high latitudes characterized by an extreme seasonality in incoming sunlight and the presence of sea-ice. Therefore, the causes of the mortality of pteropods in our study could not be determined with a certainty. Thus, we speculate and discuss environmental conditions recorded during the sampling campaign that could have potentially and additionally influence the mortality of pteropods along the transect.

There is a clear pattern within the distribution of dead shells with highest concentrations at stations (P5–P2) influenced by the PW masses (**Figures 4A,B**). At station P3 and P2, where the PW masses dominate, the lowest temperatures (–1.87), Ω_{Ar} (1.13–1.44) and pH (7.97–8.10) were recorded (**Table 1** and **Figures 4B,C**). Although, the link between low Ω_{Ar} and pH, and low temperatures conditions-driven mortality in pteropods has not been directly confirmed in nature (Gazeau et al., 2013; Bednaršek et al., 2014a; Niemi et al., 2021), our data suggest that the low values of these environmental variables may have contributed to an increased mortality of veligers at our stations. Temperature is recognized to have a strong influence on the shell building capacity of calcifying organisms and larval forms of molluscs have been shown to be particularly sensitive to changes in carbonate chemistry (Gazeau et al., 2013). Moreover, early stages of *L. helicina* in the PW during winter were found to be less able to counteract changes in their environment (Lischka et al., 2011; Lischka and Riebesell, 2012). Therefore, the combination of low temperatures, relatively low Ω_{Ar} with potentially limited food availability during winter, could have added to the adverse conditions impairing the survival capability of the larvae forms leading to increased mortality of ssL. However, more studies are needed to further examine the effects and disentangle the relative contribution of these important environmental variables for shelled pteropods.

Another explanation to the occurrence of empty shells of ssL could be as a result from predation activity by gymnosomatous (non-shelled) pteropods such as *Clione limacina* that is a highly specialized predator adapted to feed on soft body of *L. helicina* (Lalli, 1970; Conover and Lalli, 1974; Norekian and Satterlie, 1996; Böer et al., 2005). However, the low abundance of *C. limacina* found at station P5 and the absence of *C. limacina* at the remaining stations (**Figure 3A**) cannot account for the high concentrations of empty shells of ssL e.g., at stations P2 and P3. However, as *C. limacina* can use fast swimming behavior for hunting, we cannot rule out, that higher abundance of this species after exhausting the consumption potential at these stations left for other grazing areas leaving the slower sinking empty shells behind. Moreover, the low abundance of *C. limacina* could also, at least partially, result from the avoidance of the net by this species. Net avoidance by larger and more efficiently swimming zooplankton that sense the pressure wave in front of a small mesh net and therefore can dodge it, is a known phenomenon that to a large extend can be avoided by an adequate towing speed. The towing speed recommended for vertical samples with a small mesh net (63 μm), used in our study, is 0.5–1 m per second. This rater slow towing speed minimizes the extent of extrusion of small-sized foraminifera and pteropods, but may increase the likelihood of avoidance by the bigger and faster swimming *C. limacina*.

Independent from the reason of the occurrence of the high concentration of empty shells of pteropods (or planktic

foraminifera) their high concentration likely represents a substantial part of the inorganic carbonate flux to the ocean floor. This is in agreement with the findings of Manno et al. (2018) that showed that the contribution of pteropods to the carbonate counter pump depends on whether shells were empty or included soft tissue. The dominance of empty shells in the total pteropod abundance (up to 85%) in the sediment traps resulted in the contribution to the carbonate counter pump that was more than two times higher than when shells with soft tissue predominated. This strongly underlines the importance of examination of empty shells in biological carbon flux studies.

CONCLUSION

To our knowledge, this is the first study of the under-ice abundance and diversity of planktic foraminifera and shelled pteropods in the Barents Sea during dark winter to date. This is also the first presentation of carbonate and nutrient data from the northern Barents Sea in December.

The abundances of living planktic foraminifera followed a distribution similar to open ocean with maximum abundances recorded in surface waters at 0–50 m depth (2.6 ind. m^{-3} at station P7 and 5.8 ind. m^{-3} at station P6). However, the average abundance of living planktic foraminifera was generally very low for the upper 200 m water depth and never exceeded 2 ind. m^{-3} which was the maximum value recorded close to the Polar Front. The concentration of living specimens was only higher in station P5.

Similarly, to planktic foraminifera, the highest abundance of living pteropods was found in the surface water at 0–50 m depth (32 ind. m^{-3} at station P5). The average abundances of pteropods recorded in the upper 200 m water depth in December were comparable to abundances found in Barents Sea in spring and summer. Abundances of living pteropods were, however, markedly lower than the abundances of empty shells of pteropods that ranged between 6 ind. m^{-3} (P5) and 372 ind. m^{-3} (P2) in the northern Barents Sea. The high abundance of empty shells can represent a substantial part of the inorganic carbonate flux to the deep ocean in this area.

The polar pteropod species *Limacina helicina* and the polar planktic foraminifera species *Neogloboquadrina pachyderma* dominated the living pteropods and foraminifera assemblages, respectively. The high proportion of the subpolar foraminiferal species *Turborotalita quinqueloba* (45–67%) at stations in the south (P1) and in the Nansen Basin (P7 and P6) was probably linked to the presence of AW advected by the WSC. This could also explain the presence of *Limacina retroversa* at stations P6 and P5 where Atlantic water dominated. This confirms recent studies that refer to a poleward expansion of subpolar plankton communities to stronger and warmer Atlantic water currents entering the Arctic Ocean (Dalpadado et al., 2020). In a changing climate, this implies a high latitude shift toward more subpolar species. However, our study confirms the division in different regimes, between warm water subpolar species and the cold water polar species.

Limacina helicina was represented mainly by the juvenile form that showed a preference toward PW with temperatures < -0.4°C. Moreover, this species was found in water masses with the lowest Ω_{Ar}. *Limacina helicina* was represented mainly by juveniles that most likely spawned in late autumn/early winter. Its occurrence may suggest that a slow growth of the overwintering *Limacina helicina* veligers into juveniles occurred which agrees with recent studies that evidenced an active growing of *Limacina helicina antarctica* during winter in Antarctica.

Our study provides a limited "snapshot-type" observation in winter that cannot provide the full picture of the dynamics of two groups of pelagic calcifiers nor the environmental factors controlling their populations. It, however, highlights that a repeated sampling strategy covering full annual cycles would be crucial for studying long-term trends in the occurrence, abundance and population structure of planktic foraminifera and shelled pteropods to improve our understanding and prediction of their sensitivities to ocean changes.

DATA AVAILABILITY STATEMENT

The original contributions presented in the study are included in the article/**Supplementary Material**, further inquiries can be directed to the corresponding author/s.

AUTHOR CONTRIBUTIONS

KZ, AF, and MC were involved in the study design. KZ performed the sampling, analyzed the plankton net samples and created the tables and figures. HL and EJ sampled the water column for carbonate chemistry and nutrients and completed carbonate chemistry analyses. EJ, MC, and AF were involved in the carbonate chemistry calculations. GA-O contributed with measurements of individual pteropods in fraction > 500 μm. KZ completed the writing of the manuscript with contributions from AF, MC, EJ, JM, GA-O, and HL. All authors contributed to the article and approved the submitted version.

FUNDING

This study was carried out as part of the Research Council of Norway through the project "The Nansen Legacy" (RCN #276730) and within the framework of the Flagship research program "Ocean Acidification and effects in northern waters" within the FRAM - High North Research Center for Climate and the Environment at the Norwegian Polar Institute, Norway. The Geschäftsstelle Deutsche Forschungsschiffen (project 413534516) financed JM.

ACKNOWLEDGMENTS

We would like to thank the captains and crew of RV *Kronprins Haakon* and A. Wold for technical assistance and the cruise leaders J. E. Søreide and R. Gradinger for their support during

the cruise. We would like to thank B. Bye for creating the area map. We would like to appreciate Y. Ericson for helpful comments and suggestions. We would also like to thank the reviewers, Katsunori Kimoto and Brett Metcalfe, for providing helpful comments and suggestions during the review process.

SUPPLEMENTARY MATERIAL

The Supplementary Material for this article can be found online at: https://www.frontiersin.org/articles/10.3389/fmars.2021.644094/full#supplementary-material

REFERENCES

Abrahamsen, E. P., Østerhus, S., and Gammelsrød, T. (2006). Ice draft and current measurements from the north-western Barents Sea, 1993–96. *Pol. Res.* 25, 25–37. doi: 10.3402/polar.v25i1.6236

Bathmann, U. V., Noji, T. T., and Bodungen, B. V. (1991). Sedimentation of pteropods in the Norwegian Sea in autumn. *Deep-Sea Res.* 38, 1341–1360. doi: 10.1016/0198-0149(91)90031-A

Beaugrand, G., Luczak, C., and Edwards, M. (2009). Rapid biogeographical plankton shifts in the North Atlantic Ocean. *Glob. Chang. Biol.* 15, 1790–1803. doi: 10.1111/j.1365-2486.2009.01848.x

Bednaršek, N., Feely, R. A., Howes, E. L., Hunt, B., Kessouri, F., León, P., et al. (2019). Systematic review and meta-analysis towards synthesis of thresholds of ocean acidification impacts on calcifying pteropods and interactions with warming. *Front. Mar. Sci.* 6:227. doi: 10.3389/fmars.2019.00227

Bednaršek, N., Feely, R. A., Tolimieri, N., Hermann, A. J., Siedlecki, S. A., and Waldbusser, G. G. (2017). Exposure history determines pteropod vulnerability to ocean acidification along the US west coast article. *Sci. Rep.* 7:4526. doi: 10.1038/s41598-017-03934-z

Bednaršek, N., and Ohman, M. (2015). Changes in pteropod distributions and shell dissolution across a frontal system in the California Current System. *Mar. Ecol. Progress Series* 523, 93–103. doi: 10.3354/meps11199

Bednaršek, N., Mozina, J., Vogt, M., O'Brien, C., and Tarling, G. A. (2012a). The global distribution of pteropods and their contribution to carbonate and carbon biomass in the modern ocean. *Earth Sys. Sci. Data* 4, 167–186. doi: 10.5194/essd-4-167

Bednaršek, N., Tarling, G. A., Bakker, D. C. E., Fielding, S., and Feely, R. A. (2014b). Dissolution dominating calcification process in polar pteropods close to the point of aragonite undersaturation. *PLoS One* 9:e109183. doi: 10.1371/journal.pone.0109183

Bednaršek, N., Feely, R. A., Reum, J. C. P., Peterson, B., Menkel, J., Alin, S. R., et al. (2014a). *Limacina helicina* shell dissolution as an indicator of declining habitat suitability owing to ocean acidification in the California Current Ecosystem. *Proc. R. Soc. B* 281:20140123. doi: 10.1098/rspb.2014.0123

Berelson, W. M., Balch, W. M., Najjar, R., Feely, R. A., Sabine, C., and Lee, K. (2007). Relating estimates of $CaCO_3$ production, export, and dissolution in the water column to measurements of $CaCO_3$ rain ratio into sediment traps and dissolution on the sea floor: a revised global carbonate budget. *Glob. Biogeochem. Cycles* 21:GB1024. doi: 10.1029/2006GB002803

Berge, J., Daase, M., Hobbs, L., Falk-Petersen, S., Darnis, G., and Søreide, J. E. (2020). "Zooplankton in the polar night," in *Polar Night Marine Ecology. Advances in Polar Ecology*, Vol. 4, eds J. Berge, G. Johnsen, and J. Cohen (Cham: Springer).

Berner, R. A., and Honjo, S. (1981). Pelagic sedimentation of aragonite: its geochemical significance. *Science* 211, 940–942. doi: 10.1126/science.211.4485.940

Böer, M., Gannefors, C., Kattner, G., Graeve, M., Hop, H., and Falk-Petersen, S. (2005). The Arctic pteropod *Clione limacina*: seasonal lipid dynamics and life-strategy. *Mar. Biol.* 147, 707–717. doi: 10.1007/s00227-005-1607-8

Boissonnot, L., Niehoff, B., Ehrenfels, B., Søreide, J. E., Hagen, W., and Graeve, M. (2019). Lipid and fatty acid turnover of the pteropods *Limacina helicina*, *L. retroversa* and *Clione limacina* from Svalbard waters. *Mar. Ecol. Prog. Ser.* 609, 133–149. doi: 10.3354/meps12837

Brummer, G. J. A., Hemleben, C., and Spindler, M. (1986). Planktonic foraminiferal ontogeny and new perspectives for micropaleontology. *Nature* 39, 50–52. doi: 10.1038/319050a0

Buitenhuis, E. T., Le Quéré, C., Bednaršek, N., and Schiebel, R. (2019). Large contribution of pteropods to shallow $CaCO_3$ export. *Glob. Biogeochem. Cycles* 33, 458–468. doi: 10.1029/2018GB006110

Buitenhuis, E. T., van Bleijswijk, J., Bakker, D., and Veldhuis, M. (1996). Trends in inorganic and organic carbon in a bloom of *Emiliania huxleyi* in the North Sea. *Mar. Ecol. Progr. Series* 143, 271–282. doi: 10.3354/meps143271

Caromel, A. G. M., Schmidt, D. N., Fletcher, I., and Rayfield, E. J. (2016). Morphological change during the ontogeny of the planktic foraminifera. *J. Micropal.* 35, 2–19. doi: 10.1144/jmpaleo2014-017

Caromel, A. G. M., Schmidt, D. N., Phillips, J. C., and Rayfield, E. J. (2014). Hydrodynamic constraints on the evolution and ecology of planktic foraminifera. *Mar. Micropal.* 106, 69–78. doi: 10.1016/j.marmicro.2014.01.002

Caron, D. A., and Swanberg, N. R. (1990). The ecology of planktonic sarcodines. *Rev. Aquatic Sci.* 3, 147–180.

Chang, Y., and Yen, J. (2012). Swimming in the intermediate Reynolds range: kinematics of the pteropod *Limacina helicina*. *Integr. Comp. Biol.* 52, 597–615. doi: 10.1093/icb/ics113

Chierici, M., and Fransson, A. (2009). $CaCO_3$ saturation in the surface water of the Arctic Ocean: undersaturation in freshwater influenced shelves. *Biogeosciences* 6, 2421–2432. doi: 10.5194/bg-6-2421-2009

Chierici, M., Fransson, A., and Anderson, L. G. (1999). Influence of m-cresol purple indicator additions on the pH of seawater samples: correction factors evaluated from a chemical speciation model. *Mar. Chem.* 65, 281–290. doi: 10.1016/S0304-4203(99)00020-1

Chierici, M., Fransson, A., Lansard, B., Miller, L. A., Mucci, A., Shadwick, E., et al. (2011). Impact of biogeochemical processes and environmental factors on the calcium carbonate saturation state in the Circumpolar Flaw Lead in the Amundsen Gulf, Arctic Ocean. *J. Geophys. Res.* 116:C00G09. doi: 10.1029/2011JC007184

Chierici, M., Vernet, M., Fransson, A., and Børsheim, K. Y. (2019). Net community production and carbon exchange from winter to summer in the Atlantic Water inflow to the Arctic Ocean. *Front. Mar. Sci.* 6:528. doi: 10.3389/fmars.2019.00528

Clayton, T. D., and Byrne, R. H. (1993). Spectrophotometric seawater pH measurements: total hydrogen ion concentration scale calibration of m-cresol purple and at-sea results. *Deep-Sea Res. I* 40, 2115–2129. doi: 10.1016/0967-0637(93)90048-8

Comeau, S., Alliouane, S., and Gattuso, J. P. (2012). Effects of ocean acidification on overwintering juvenile Arctic pteropods *Limacina helicina*. *Mar. Ecol. Prog. Series* 456, 279–284. doi: 10.3354/meps09696

Comeau, S., Gattuso, J.-P., Nisumaa, A.-M., and Orr, J. (2011). Impact of aragonite saturation state changes on migratory pteropods. *Proc. R. Scociety Lond. Series B. Biological Sci* 279, 732–738. doi: 10.1098/rspb.2011.0910

Comeau, S., Gorsky, G., Jeffree, R., Teyssie, J. L., and Gatusso, J. P. (2009). Impact of ocean acidification on a key Arcticpelagic mollusc (*Limacina helicina*). *Biogeosciences* 6, 1877–1882. doi: 10.5194/bg-6-1877-2009

Comeau, S., Jeffree, R., Teyssié, J.-L., and Gattuso, J.-P. (2010). Response of the arctic pteropod *Limacina helicina* to projected future environmental conditions. *PLoS One* 5:e11362. doi: 10.1371/journal.pone.0011362

Conover, R. J., and Lalli, C. M. (1974). Feeding and growth in *Clione limacine* (Phipps), a pteropod mollusc. II. Assimilation, metabolism and growth efficiency. *J. Exp. Mar. Biol. Ecol.* 16, 131–154. doi: 10.1016/0022-0981(74)90016-1

Daase, M., and Eiane, K. (2007). Mesozooplankton distribution in northern Svalbard waters in relation to hydrography. *Polar Biol.* 30, 969–981. doi: 10.1007/s00300-007-0255-5

Dalpadado, P., Arrigo, K. R., van Dijken, G. L., Skjoldal, H. R., Bagøien, E., Dolgov, A. V., et al. (2020). Climate effects on temporal and spatial dynamics of phytoplankton and zooplankton in the Barents Sea. *Prog. Oceanogr.* 185:102320. doi: 10.1016/j.pocean.2020.102320

Deser, C., Walsh, J., and Timlin, M. (2000). Arctic sea ice variability in the context of recent atmospheric circulation trends. *J. Clim.* 13, 607–633. doi: 10.1175/1520-04422000013<0617:ASIVIT<2.0.CO;2

Dickson, A. G. (1990). Standard potential of the reaction: AgCl(s) + 1/2H2 (g)=Ag(s)+ HCl(aq), and the standard acidity constant of the ion HSO4- in synthetic sea water from 273.15 to 318.15 K. *J. Chem. Thermodynam.* 22, 113–127. doi: 10.1016/0021-9614(90)90074-Z

Dickson, A. G., and Millero, F. J. (1987). A comparison of the equilibrium constants for the dissociation of carbonic acid in seawater media. *Deep-Sea Res. A* 34, 1733–1743. doi: 10.1016/0198-0149(87)90021-5

Dickson, A. G., Sabine, C. L., and Christian, J. R. (2007). *Guide to Best Practices for Ocean CO_2 Measurements. PICES Special Publication 3*. IOCCP Report 8. Sidney: North Pacific Marine Science Organization.

Dieckmann, G. S., Spindler, M., Lange, M. A., Ackley, S. F., and Eicken, H. (1991). Antarctic sea ice: a habitat for the foraminifer *Neogloboquadrina pachyderma*. *J. Foram. Res.* 21, 182–189. doi: 10.2113/gsjfr.21.2.182

Divine, D. D., and Dick, C. (2006). Historical variability of sea ice edge position in the Nordic Seas. *J. Geophys. Res.* 111:C01001. doi: 10.1029/2004JC002851

Fabry, V. J., Seibel, B. A., Feely, R. A., and Orr, J. C. (2008). Impacts of ocean acidification on marine fauna and ecosystem processes. *ICES J. Mar. Sci.* 65, 414–432. doi: 10.1093/icesjms/fsn048

Falk-Petersen, S., Leu, E., Berge, J., Kwasniewski, S., Nygård, H., Røstad, A., et al. (2008). Vertical migration in high Arctic waters during autumn 2004. *Deep Sea Res. II, Topical Stud. Oceanogr.* 55, 2275–2284. doi: 10.1016/j.dsr2.2008.05.010

Fransson, A., Chierici, M., Skjelvan, I., Olsen, A., Assmy, P., Peterson, A. K., et al. (2017). Effects of sea-ice and biogeochemical processes and storms on under-ice water fCO_2 during the winter-spring transition in the high Arctic Ocean: implications for sea-air CO_2 fluxes. *J. Geophys. Res. Oceans* 122, 5566–5587. doi: 10.1002/2016JC012478

Gannefors, C., Böer, M., Kattner, G., Graeve, G., Eiane, K., Gulliksen, B., et al. (2005). The Arctic sea butterfly *Limacina helicina*: lipids and life strategy. *Mar. Biol.* 147, 169–177. doi: 10.1007/s00227-004-1544-y

Gazeau, F., Parker, L. M., Comeau, S., Gattuso, J.-P., O'Connor, W. A., Martin, S., et al. (2013). Impacts of ocean acidification on marine shelled molluscs. *Mar. Biol.* 160, 2207–2245. doi: 10.1007/s00227-013-2219-3

Gradinger, R., and Ikävalko, J. (1998). Organism incorporation into newly forming Arctic sea ice in the Greenland Sea. *J. Plankton Res.* 20, 871–886. doi: 10.1093/plankt/20.5.871

Grasshof, K., Kremling, K., and Ehrhardt, M. (2009). *Methods of Sea-Water Analysis*, 3rd Edn. New York, NY: John Wiley.

Heinze, C., Maier-Reimer, E., and Winn, K. (1991). Glacial pCO_2 reduction by the World Ocean: experiments with the Hamburg carbon cycle model. *Paleoceanography* 6, 395–430. doi: 10.1029/91PA00489

Howard, W. R., Roberts, D., Moy, A. D., Lindsay, M. C. M., Hopcroft, R. R., Trull, T. W., et al. (2011). Distribution, abundance and seasonal flux of pteropods in the Sub-Antarctic Zone. *Deep Sea Res. II* 58, 2293–2300. doi: 10.1016/j.dsr2.2011.05.031

Hunt, B. P., Strugnell, J., Bednaršek, N., Linse, K., Nelson, R. J., Pakhomov, E., et al. (2010). Poles apart: the bipolar pteropod species *Limacina helicina* is genetically distinct between the Arctic and Antarctic oceans. *PLoS One* 5:e9835. doi: 10.1371/journal.pone.0009835

Hunt, B. P. V., Pakhomov, E. A., Hosie, G. W., Siegel, V., Ward, P., and Bernard, K. S. (2008). Pteropods in southern ocean ecosystems. *Prog. Oceanogr.* 78, 193–221. doi: 10.1016/j.pocean.2008.06.001

Kacprzak, P., Panasiuk, A., Wawrzynek, J., and Weydmann, A. (2017). Distribution and abundance of pteropods in the western Barents Sea. *Oceanol. Hydrobiol. Stud.* 46, 393–404. doi: 10.1515/ohs-2017-0039

Kobayashi, H. A. (1974). Growth cycle and related vertical distribution of the thecosomatous pteropod spiratella ("*Limacina*") *helicina* in the Central Arctic Ocean. *Mar. Biol.* 26, 295–301. doi: 10.1007/BF00391513

Krembs, C., Eicken, H., Junge, K., and Deming, J. W. (2002). High concentrations of exopolymeric substances in Arctic winter sea ice: implications for the polar ocean carbon cycle and cryoprotection of diatoms. *Deep-Sea Res. I* 49, 2163–2181. doi: 10.1016/S0967-0637(02)00122-X

Kretschmer, K., Kucera, M., and Schulz, M. (2016). Modeling the distribution and seasonality of *Neogloboquadrina pachyderma* in the North Atlantic Ocean during Heinrich Stadial 1. *Paleoceanogr. Paleoclimatol.* 31, 986–1010. doi: 10.1002/2015PA002819

Kroeker, K., Kordas, R., Crim, R., and Singh, G. (2010). Meta-analysis reveals negative yet variable effects of ocean acidification on marine organisms. *Ecol. Lett.* 13, 1419–1434. doi: 10.1111/j.1461-0248.2010.01518.x

Kucera, M., Weinelt, M., Kiefer, T., Pflaumann, U., Hayes, A., Weinelt, M., et al. (2005). Reconstruction of sea-surface temperatures from assemblages of planktonic foraminifera: multi-technique approach based on geographically constrained calibration data sets and its application to glacial Atlantic and Pacific Oceans. *Quat. Sci. Rev.* 24, 951–998. doi: 10.1016/j.quascirev.2004.07.014

Kuhnt, T., Howa, H., Schmidt, S., Marié, L., and Schiebel, R. (2013). Flux dynamics of planktic foraminiferal tests in the south-eastern Bay of Biscay (northeast Atlantic margin). *J. Mar. Sys.* 109–110, 169–181. doi: 10.1016/j.jmarsys.2011.11.026

Kushnir, V. M., Hansen, E., Petrenko, L. A., Pavlov, V. K., Morozov, A. N., Stanichnyi, S. V., et al. (2007). Currents and turbulent diffusion in the bottom boundary layer of the Barents Sea. *Phys. Oceanogr.* 17, 278–295. doi: 10.1007/s11110-007-0022-8

Lalli, C. M. (1970). Structure and function of the buccal apparatus of *Clione limacina* (Phipps) with a review of feeding in gymnosomatous pteropods. *J. Exp. Mar. Biol. Ecol.* 4, 101–118. doi: 10.1016/0022-0981(70)90018-3

Lalli, C. M., and Gilmer, R. W. (1989). *Pelagic Snails: the Biology of Holoplanktonic Gastropod Mollusks*. Santa Clara, CA: Stanford University Press, Palo Alto, 259.

Lee, K., Kim, T.-W., Byrne, R. H., Millero, F. J., Feely, R. A., and Liu, Y.-M. (2010). The universal ratio of boron to chlorinity for the North Pacific and North Atlantic oceans. *Geochim. Cosmochim. Acta* 74, 1801–1811. doi: 10.1016/j.gca.2009.12.027

Lien, V. S., and Trofimov, A. G. (2013). Formation of Barents Sea branch water in the north-eastern Barents Sea. *Polar Res.* 32:18905. doi: 10.3402/polar.v32i0.18905

Lind, S., and Ingvaldsen, R. B. (2012). Variability and impacts of Atlantic Water entering the Barents Sea from the north. *Deep Sea Res. I* 62, 70–88. doi: 10.1016/j.dsr.2011.12.007

Lischka, S., Büdenbender, J., Boxhammer, T., and Riebesell, U. (2011). Impact of ocean acidification and elevated temperatures on early juveniles of the polar shelled pteropod *Limacina helicina*: mortality, shell degradation, and shell growth. *Biogeosciences* 8, 919–932. doi: 10.5194/bg-8-919-2011

Lischka, S., and Riebesell, U. (2012). Synergistic effects of ocean acidification and warming on overwintering pteropods in the Arctic. *Glob. Chang. Biol.* 18, 3517–3528. doi: 10.1111/gcb.12020

Loeng, H. (1991). Features of the physical oceanographic conditions in the Barents Sea. *Polar Res.* 10, 5–18. doi: 10.3402/polar.v10i1.6723

Maas, A. E., Wishner, K. F., and Seibel, B. A. (2012). The metabolic response of pteropods to acidification reflects natural CO_2-exposure in oxygen minimum zones. *Biogeosciences* 9, 747–757. doi: 10.5194/bg-9-747-2012

Manno, C., Bednarsek, N., Tarling, G. A., Peck, V. L., Comeau, S., Adhikari, D., et al. (2017). Shelled pteropods in peril: assessing vulnerability in a high CO_2 ocean. *Earth Sci. Rev.* 169, 132–145. doi: 10.1016/j.earscirev.2017.04.005

Manno, C., Giglio, F., Stowasser, G., Fielding, S., Enderlein, P., and Tarling, G. (2018). Threatened species drive the strength of the carbonate pump in the northern Scotia Sea. *Nat. Commun.* 9:4592. doi: 10.1038/s41467-018-07088-y

Manno, C., Morata, N., and Bellerby, R. (2012a). Effect of ocean acidification and temperature increase on the planktonic foraminifer *Neogloboquadrina pachyderma* (sinistral). *Polar Biol.* 35, 1311–1319. doi: 10.1007/s00300-012-1174-7

Manno, C., Morata, N., and Primicerio, R. (2012b). *Limacina retroversa*'s response to combined effects of ocean acidification and sea water freshening. *Estuar. Coast. Shelf Sci.* 113, 163–171. doi: 10.1016/j.ecss.2012.07.019

Marszalek, D. S. (1982). The role of heavy skeletons in vertical movements of non-motile zooplankton. *Mar. Behav. Physiol.* 8, 295–303. doi: 10.1080/10236248209387026

Mehrbach, C., Culberson, C. H., Hawley, J. E., and Pytkowicz, R. M. (1973). Measurement of the apparent dissociation constants of carbonic acid in seawater at atmospheric pressure. *Limnol. and Oceanog.* 18, 897–907. doi: 10.4319/lo.1973.18.6.0897

Meilland, J., Howa, H., Hulot, V., Demangel, I., Salaün, J., and Garlan, T. (2020). Population dynamics of modern planktonic foraminifera in the western Barents Sea. *Biogeosciences* 17, 1437–1450. doi: 10.5194/bg-17-1437-2020

Meilland, J., Schiebel, R., Monaco, C. L., Sanchez, S., and Howa, H. (2018). Abundances and test weights of living planktic foraminifers across the Southwest Indian Ocean: implications for carbon fluxes. *Deep-Sea Res. I* 131, 27–40. doi: 10.1016/j.dsr.2017.11.004

Millero, F. J. (1979). The thermodynamics of the carbonate system in seawater. *Geochim. Cosmochim. Acta* 43, 1651–1661. doi: 10.1016/0016-7037(79)90184-4

Milliman, J. D. (1993). Production and accumulation of calcium carbonate in the ocean: budget of a nonsteady state. *Glob. Biogeochem. Cycles* 7, 927–957. doi: 10.1029/93GB02524

Mosby, H. (1938). Svalbard waters. *Geofysiske Publikasjoner* 124, 1–85.

Moy, A., Howard, W., Bray, S., and Trull, T. (2009). Reduced calcification in modern southern ocean planktonic foraminifera. *Nat. Geosci.* 2, 276–280. doi: 10.1038/ngeo460

Mucci, A. (1983). The solubility of calcite and aragonite in seawater at various salinities, temperatures, and one atmosphere total pressure. *Am. J. Sci.* 283, 780–799. doi: 10.2475/ajs.283.7.780

Murray, J. W. (1991). "Ecology and distribution of benthic foraminifera," in *Biology of Foraminifera*, eds J. J. Lee and R. Anderson (Cambridge, MA: Academic Press Limited), 221–253.

Niemi, A., Bednaršek, N., Michel, C., Feely, R. A., Williams, W., Azetsu-Scott, K., et al. (2021). Biological impact of ocean acidification in the Canadian Arctic: widespread severe pteropod shell dissolution in Amundsen Gulf. *Front. Mar. Sci.* 8:600184. doi: 10.3389/fmars.2021.600184

Nigam, R., Saraswat, R., and Mazumder, A. (2003). Life spans of planktonic foraminifers: new sight through sediment traps. *J. Palaeontol. Soc. Ind.* 48, 129–133.

Norekian, T. P., and Satterlie, R. A. (1996). Whole body withdrawal circuit and its involvement in the behavioral hierarchy of the mollusk *Clione limacina*. *J. Neurophysiol.* 75, 529–537. doi: 10.1152/jn.1996.75.2.529

Ofstad, S., Meilland, J., Zamelczyk, K., Chierici, M., Fransson, A., Gründger, F., et al. (2020). Development, productivity, and seasonality of living planktonic foraminiferal faunas and *Limacina helicina* in an area of intense methane seepage in the Barents Sea. *J. Geoph. Res. Biogeosci.* 125:e2019JG005387. doi: 10.1029/2019JG005387

Pados, T., and Spielhagen, R. F. (2014). Species distribution and depth habitat of recent planktic foraminifera in Fram Strait, Arctic Ocean. *Pol. Res.* 33:22483. doi: 10.3402/polar.v33.22483

Pasternak, A. F., Drits, A. V., and Flint, M. V. (2017). Feeding, egg production, and respiration rate of pteropods *Limacina* in Arctic seas. *Oceanology* 57, 122–129. doi: 10.1134/S000143701701012X

Percy, J. A., and Fife, F. J. (1985). Energy distribution in an Arctic coastal macrozooplankton community. *Arctic* 38, 39–42.

Pfirman, S. L., Bauch, D., and Gammelsrød, T. (1994). "The northern Barents Sea: water mass distribution and modification," in *The Polar Oceans and their Role in Shaping the Global Environment*, Vol. 85, eds O. M. Johannesen, R. D. Muench, and J. E. Overland (Washington, DC: AGU), 77–94.

Pierrot, D., Lewis, E., and Wallace, D. W. R. (2006). *MS Excel Program Developed for CO_2 system Calculations, ORNL/CDIAC-105, Carbon Dioxide Information Analysis Center, Oak Ridge National Laboratory, US Department of Energy*. Oak Ridge: US Department of Energy.

Reigstad, M., Wassmann, P., Wexels Riser, C. H., Oygarden, S., and Rey, F. (2002). Variations in hydrography, nutrients and chlorophyll *a* in the marginal ice-zone and the central Barents Sea. *J. Mar. Sys.* 38, 9–29. doi: 10.1016/S0924-7963(02)00167-7

Riley, J. P., and Tongudai, M. (1967). The major cation/chlorinity ratios in sea water. *Chem. Geol.* 2, 263–269. doi: 10.1016/0009-2541(67)90026-5

Rudels, B., Anderson, L. G., and Jones, E. P. (1996). Formation and evolution of the surface mixed layer and halocline of the Arctic Ocean. *J. Geophys. Res.* 101, 8807–8821. doi: 10.1029/96JC00143

Rudels, B., Jones, E. P., Schauer, U., and Eriksson, P. (2004). Atlantic sources of the Arctic Ocean surface and halocline waters. *Polar Res.* 23, 181–208. doi: 10.1111/j.1751-8369.2004.tb00007.x

Schiebel, R. (2002). Planktic foraminiferal sedimentation and the marine calcite budget. *Global Biogeochem. Cycles* 16:1065. doi: 10.1029/2001GB001459

Schiebel, R., and Hemleben, C. (2017). *Planktic Foraminifers in the Modern Ocean*. Berlin: Springer-Verlag GmbH, 357.

Schmuker, B. (2000). The influence of shelf vicinity on the distribution of planktic foraminifera south of Puerto Rico. *Mar. Geol.* 166, 125–143. doi: 10.1016/S0025-3227(00)00014-1

Seibel, B. A., and Dierssen, H. M. (2003). Cascading trophic impacts of reduced biomass in the Ross Sea, Antarctica: just the tip of the Iceberg? *Biol. Bull.* 205, 93–97.

Seibel, B. A., Dymowska, A., and Rosenthal, J. (2007). Metabolic temperature compensation and coevolution of locomotory performance in pteropod molluscs. *Integrat. Comparat. Biol.* 47, 880–891. doi: 10.1093/icb/icm089

Seibel, B. A., Maas, A. E., and Dierssen, H. M. (2012). Energetic plasticity underlies a variable response to ocean acidification in the pteropod, *Limacina helicina antarctica*. *PLoS One* 7:e30464. doi: 10.1371/journal.pone.0030464

Shadwick, E. H., Thomas, H., Chierici, M., Else, B., Fransson, A., Michel, C., et al. (2011). Seasonal variability of the inorganic carbon system in the Amundsen Gulf region of the southeastern Beaufort Sea. *Limnol. Oceanogr.* 56, 303–322. doi: 10.4319/lo.2011.56.1.0303

Shapiro, I., Colony, R., and Vinje, T. (2003). April sea ice extent in the Barents Sea, 1850–2001. *Polar Res.* 22, 5–10. doi: 10.3402/polar.v22i1.6437

Spindler, M. (1996). On the salinity tolerance of the planktonic foraminifer *Neogloboquadrina pachyderma* from antarctic sea ice. *Proc. NIPR Sympos. Polar Biol.* 9, 85–91.

Steinacher, M., Joos, F., Frölicher, T. L., Plattner, G.-K., and Doney, S. C. (2009). Imminent ocean acidification in the Arctic projected with the NCAR global coupled carbon cycle-climate model. *Biogeosciences* 6, 515–533. doi: 10.5194/bg-6-515-2009

Sundfjord, A., Assmann, K. M. Lundesgaard, ø., Renner, A. H. H., Lind, S., and Ingvaldsen, R. B. (2020). *Suggested Water Mass Definitions for the Central and Northern Barents Sea, and the Adjacent Nansen Basin: Workshop Report. Nansen Legacy Report Series 8/2020*. Tromsø: The Arctic University of Norway. doi: 10.7557/nlrs.5707

Takahashi, K., and Bé, A. W. H. (1984). Planktonic foraminifera: factors controlling sinking speeds. *Deep Sea Res. A. Oceanogr. Res. Pap.* 31, 1477–1500. doi: 10.1016/0198-0149(84)90083-9

Thibodeau, P. S., Steinberg, D. K., McBride, C. E., Conroy, J. A., Keul, N., and Ducklow, H. W. (2020). Long-term observations of pteropod phenology along the Western Antarctic Peninsula. *Deep Sea Res. I. Oceanogr. Res. Pap.* 166:103363. doi: 10.1016/j.dsr.2020.103363

Tynan, E., Clarke, J. S., Humphreys, M. P., Ribas-Ribas, M., Esposito, M., Rérolle, V. M. C., et al. (2016). Physical and biogeochemical controls on the variability in surface pH and calcium carbonate saturation states in the Atlantic sectors of the Arctic and Southern Oceans 2016. *Deep Sea Res.* II 127, 7–27. doi: 10.1016/j.dsr2.2016.01.001

Tyrrell, T. (2008). Calcium carbonate cycling in future oceans and its influence on future climates. *J. Plank. Res.* 30, 141–156. doi: 10.1093/plankt/fbm105

van Der Spoel, S. (1967). *Euthecosomata, a Group with Remarkable Developmental Stages (Gastropoda, Pteropoda)*. Utrecht: Bohn, Scheltema & Holkema, 375.

van Der Spoel, S. (1976). *Pseudothecosomata, Gymnosomata and Heteropoda (Gastropoda)*. Utrecht: Bohn, Scheltema, and Holkema, 484.

Vinje, T. (2001). Anomalies and trends of sea-ice extent and atmospheric circulation in the Nordic Seas during the period 1864–1998. *J. Clim.* 14, 255–267. doi: 10.1175/1520-0442(2001)014<0255:AATOSI>2.0.CO;2

Volk, T., and Hoffert, M. I. (1985). "Ocean carbon pumps: Analysis of relative strengths and efficiencies in ocean-driven atmospheric CO_2 changes," in *The Carbon Cycle and Atmospheric CO_2: Natural Variations Archean to Present*, eds E. Sundquist and W. S. Broecker (Washington: American Geophysical Union).

Volkmann, R. (2000). Planktic foraminifers in the outer Laptev Sea and the Fram Strait modern distribution and ecology. *J. Foramini. Res.* 30, 157–176. doi: 10.2113/0300157

Von Gyldenfeldt, A. B., Carstens, J., and Meincke, J. (2000). Estimation of the catchment area of a sediment trap by means of current meters and foraminiferal tests. *Deep-Sea Res. II* 47, 1701–1717. doi: 10.1016/S0967-0645(00)00004-7

Walker, M., Hammel, J. U., Wilde, F., Hoehfurtner, T., Humphries, S., and Schuech, R. (2021). Estimation of sinking velocity using free-falling dynamically scaled models: foraminifera as a test case. *J. Exp. Biol.* 224:jeb230961. doi: 10.1242/jeb.230961

Wang, K., Hunt, B. P. V., Liang, C., Pauly, D., and Pakhomov, E. A. (2017). Reassessment of the life cycle of the pteropod *Limacina helicina* from a high resolution interannual time series in the temperate North Pacific. *ICES J. Mar. Sci.* 74, 1906–1920. doi: 10.1093/icesjms/fsx014

Wassmann, P., Carmack, E., Slagstad, D., Kosobokova, K., Drinkwater, K., Ellingsen, I., et al. (2015). The contiguous domains of Arctic Ocean advection: trails of life and death. *Prog. Oceanogr.* 139, 42–65. doi: 10.1016/j.pocean.2015.06.011

Watanabe, E., Onodera, J., Harada, N., Honda, M. C., Kimoto, K., Kikuchi, T., et al. (2014). Enhanced role of eddies in the Arctic marine biological pump. *Nature Comm.* 5:3950. doi: 10.1038/ncomms4950

Werner, I. (2005). Living conditions abundance and biomass of under-ice fauna in the Storfjord area (western Barents Sea, Arctic) in late winter (March 2003). *Polar Biol.* 28, 311–318. doi: 10.1007/s00300-004-0678-1

Zeebe, R., and Wolf-Gladrow, D. (2001). *CO2 in Seawater: Equilibrium, Kinetics, Isotopes. Elsevier Oceanography Series*. Amsterdam: Elsevier, 65.

Conflict of Interest: The authors declare that the research was conducted in the absence of any commercial or financial relationships that could be construed as a potential conflict of interest.

Publisher's Note: All claims expressed in this article are solely those of the authors and do not necessarily represent those of their affiliated organizations, or those of the publisher, the editors and the reviewers. Any product that may be evaluated in this article, or claim that may be made by its manufacturer, is not guaranteed or endorsed by the publisher.